Characterization of Na^+ Permeation and Block of hERG Potassium Channels

by

Hongying Gang

A Thesis submitted to the Faculty of Graduate Studies of

The University of Manitoba

in partial fulfilment of the requirements of the degree of

MASTER OF SCIENCE

Department of Physiology

University of Manitoba

Winnipeg

THE UNIVERSITY OF MANITOBA

FACULTY OF GRADUATE STUDIES

*****

COPYRIGHT PERMISSION

Characterization of Na^+ Permeation and Block of hERG Potassium channels

BY

Hongying Gang

A Thesis/Practicum submitted to the Faculty of Graduate Studies of The University of Manitoba in partial fulfillment of the requirement of the degree

OF

Master of Science

TABLE OF CONTENTS

ACKNOWLEDGEMENTS

I would like to express my sincere gratitude to my supervisor, Dr. Shetuan Zhang for his guidance, support and providing me with the opportunity to study in the electrophysiology field. He has been a constant presence throughout my graduate program, always available to answer questions, provide insights and share ideas. Besides, I thank him for supporting me to finish the thesis successfully and on time.

I extend my appreciation to my committee members, Dr. Hryshko, Dr. Netticadan and Dr. Wigle for their guidance and for taking the time to meet with me throughout the year to discuss the outcomes of my project. Thank you for providing me with important insights, useful critiques, valuable comments and suggestions.

This work would not have been completed without the help of the current and former members of the lab. Thank you to Jun Guo, my friend, for teaching me step-by-step through the patch clamp techniques and for helping me record those beautiful currents. Thank you for maintaining and preparing excellent cells for patch clamp recording. Thank you to Wentao Li, for assisting me in acquiring the considerable amounts of data used in the thesis. Thank you to Ms. Jianmin Xu, Ms. Tonghua Yang, Mr. Tao Luo, Ms. Min Liu and Dr. Harsurinder Mavi for your comraderie, your patience, and your eagerness to help me through both the good and tough times.

Special thanks to those in other labs who provided assistance and answered questions: Dr. Dhalla Naranjan, Ms. Harjot Saini, Mr. Raja Singh, Mr. Vijayan Elimban, Mr. Donald Chapman, Dr. Shumei Ma, Dr. Xie and Dr. Barbara Triggs-Raine, the department office stuff, all of my excellent professors and my fellow graduate students.

Last but not the least, I would like to thank my parents for encouraging me to reach for my goals and always being proud of me for what I accomplish. The biggest thanks goes to my husband, Hongzhao Li, whose unconditional love, unyielding support and unremitting commitment carried me through from beginning to end.

LIST OF ABBREVIATIONS

EAG.....Ether-a-go-go

ECG.....Electrocardiogram

hERG.....Human ether-a-go-go-related gene

HEK.....Human embryonic kidney

I^c.....'C-type' inactivation

IC_{50}.....Half maximal-inhibitory concentration

I^p.....P-type inactivation

I_{Kr}.....Rapidly activating delayed rectifier K^+ current

I_{Ks}.....Slow delayed rectifier K^+ current

K_V channels.....Voltage-gated K^+ channels

LQTS.....Long QT syndrome

MEM.....Minimum essential medium

NMG^+.....N-Methyl-D-glucamine

PAS.....Per-Amt-Sim

TdP.....Torsade de pointes

TEA^+.....Tetraethylammonium

WT.....Wild type

LIST OF FIGURES

ABSTRACT

The inactivation gating of hERG channels is important for channel function and drug-channel interactions. Whereas open hERG channels are highly selective for K^+, we have found that inactivated hERG channels allow Na^+ to permeate in the absence of K^+. This provides a novel way to directly monitor and investigate hERG inactivation. By using the whole cell patch clamp method with an internal solution containing 135 mM Na^+ and an external solution containing 135 mM NMG^+, we recorded a robust Na^+ current through hERG channels expressed in HEK 293 cells. Kinetic analyses of the hERG Na^+ and K^+ currents indicate that the channel experiences at least two states during the inactivation process, an initial fast, less stable state followed by a slow, more stable state. The Na^+ current reflects Na^+ ions permeating through the fast inactivated state but not through either the slow inactivated state or open state. Thus, the hERG Na^+ current displayed a slow inactivation as the channels travel from the less stable, fast inactivated state into the more stable, slow inactivated state. Removal of fast inactivation by the S631A mutation abolished the Na^+ current. Moreover, acceleration of fast inactivation by mutations T623A, F627Y and S641A did not affect the hERG Na^+ current, but greatly diminished the hERG K^+ current. We also found that external Na^+ potently blocked the hERG outward Na^+ current with an IC_{50} of 3.5 mM. Mutations in the channel pore and S6 regions, such as S624A, F627Y, and S641A, abolished the inhibitory effects of external Na^+ on the hERG Na^+ current. Na^+ permeation and blockade of hERG channels provide novel ways to extend our understanding of the hERG channel gating mechanisms.

I. INTRODUCTION

hERG (**h**uman **e**ther-a-go-go-**r**elated **g**ene) encodes a voltage-gated K^+ channel that is expressed in a number of cell types including neurons, cardiac myocytes and tumor cells (Sanguinetti et al., 1995; Trudeau et al., 1995; Faravelli et al., 1996; Bianchi et al., 1998). In the heart, hERG channels conduct the rapidly activating delayed rectifier K^+ current (I_{Kr}) which is important for cardiac repolarization (Sanguinetti and Jurkiewicz, 1990b; Sanguinetti et al., 1995). Reduction of I_{Kr} due to mutations in hERG or drug block slows repolarization, causing long QT syndrome (LQTS) and sudden cardiac death (Keating and Sanguinetti, 2001).

The hERG K^+ channel belongs to the voltage gated K^+ channel superfamily. Thus, the opening of the channel is induced by cell membrane depolarization. Once open, hERG channel's conductance reduces even though the activating voltage is maintained. This reduction in conductance during the maintained activating voltage is called inactivation. The inactivation of hERG channels is fast and strongly voltage dependent. The inactivation of hERG is of physiological and pharmacological significance. Physiologically, the fast voltage-dependent inactivation limits outward current through the channel at positive voltages and thus helps maintain the action potential plateau phase that controls contraction and prevents premature excitation. Pharmacologically, hERG inactivation gating is involved in high affinity binding of many diverse drugs to the channel. Despite its importance, the inactivation of hERG is currently not well understood.

The inactivation of hERG channels resembles the C-type inactivation of *Shaker* K^+ channels in its sensitivity to extracellular K^+ concentration and TEA^+, and to mutations in the P-loop (Hoshi et al., 1991; Smith et al., 1996; Schönherr and Heinemann, 1996; Fan et al., 1999). The C-type inactivation of K^+ channels is not well understood, and seems to involve either multiple mechanisms or a single mechanism with multiple steps (Olcese et al., 1997; Yang et al., 1997b; Loots and Isacoff, 1998; Kiss et al., 1999; Wang and Fedida, 2001). For example, Loots *et al.* has shown that C-type inactivation involves a faster closing of the channel pore and a much slower gating charge immobilization (Loots et al., 1998). To describe the complexity of the C-type inactivation process, the term P-type inactivation has been used to refer to the initial closure of the channel pore, and the term 'C-type inactivation' has been assigned to specifically mean the stabilized inactivated conformation of the channel (De Biasi et al., 1993; Loots et al., 1998). In this concept, P-type inactivation appears to occur in a limited region of the channel pore and eliminate K^+ current without inducing substantial conformational changes in the channel. Recently, Berneche and Roux showed that the selectivity filter of the K^+ channel can undergo a transition involving two amide planes of one subunit (Val76-Gly77 and Thr75-Val76 in KcsA), which breaks the 4-fold symmetry of the tetrameric channel and contributes to the channel inactivation (Berneche and Roux, 2005). It has been shown that gating charge of 'P-type inactivated' channels is not immobilized (Yang et al., 1997b). 'C-type inactivation' may reflect a stabilized P-type inactivation, involving a further conformational change of the channel pore that stabilizes the S4 segments in the activated or outward position (Olcese et al., 1997; Wang et al., 2001). Consistent with this notion, Yang *et al.* presented evidence that P- and 'C-type' inactivations are different

from each other (Yang et al., 1997b). They showed that the 'non-conducting' W434F *Shaker* mutant is in a permanently inactivated state (P-type) but not in a permanently charge-immobilized ('C-type') state. However, most data of ionic current analyses from Kv channels are not sufficient to differentiate P- from 'C-type inactivation' because both of them are non-K^+ conducting states.

Studies on *Shaker*, Kv2.1 and Kv1.5 K^+ channels have revealed that these channels become Na^+ permeable during inactivation in the absence of K^+ (Korn and Ikeda, 1995; Starkus et al., 1997b; Starkus et al., 1998; Kiss et al., 1999; Wang et al., 2000). It has been proposed that during C-type inactivation the channels undergo three conformational states: an initial open state that is highly selective for K^+, an intermediate inactivation state that is less permeable to K^+ but more permeable to Na^+, and a final more stable inactivation state that is nonconducting (Loots et al., 1998; Starkus et al., 1997b; Kiss et al., 1999; Wang et al., 2000; Wang et al., 2001). Since hERG inactivation resembles the C-type inactivation of *Shaker* channels (Hoshi et al., 1991; Smith et al., 1996; Spector et al., 1996; Schönherr et al., 1996), we proposed that the hERG channel allows Na^+ to permeate during the inactivation process. With an intracellular solution containing 135 mM Na^+ and an extracellular solution containing 135 mM membrane-impermeable NMG^+, we have recorded a robust Na^+ current. Gating kinetic and mutational analyses suggested that the hERG channels undergo at least two inactivation steps. The less stable, P-type inactivated state is quickly reached upon depolarization, and is followed by a slow entry into the more stable 'C-type' inactivated state. The P-type inactivated state is the Na^+ permeating state, while the 'C-type' inactivated state is nonconducting. Since

inactivated channels are not K^+ permeable, directly monitoring inactivated hERG channels by Na^+ permeation would provide a novel way to extend our understanding to hERG function and drug-hERG interactions.

II. LITERATURE REVIEW

1. Introduction

HERG (human ether-a-go-go-related gene) was cloned from human brain in 1994 (Warmke and Ganetzky, 1994). This discovery can be traced back to the study of a funny behavior of the mutant *Drosophila*. Flies with a K^+ channel mutant phenotype exhibited a twitching behavior that resembled the action of a go-go dancer when the flies were anaesthetized with ether. Thus the mutant phenotype was called ether-a-go-go (EAG) (Kaplan and Trout, III, 1969). Studies of heteroexpressed EAG in frog oocytes indicated that EAG encodes a functional K^+ channel (Bruggemann et al., 1993; Ludwig et al., 1994). Soon after, Barry Ganetzky and Jeff Warmke screened a human hippocampal cDNA library and found an EAG-like gene expressed in human tissue, which was named hERG, **h**uman **E**AG-**r**elated **g**ene (Warmke et al., 1994). It soon became the focus of research interest since inherited mutations in hERG was found to cause chromosome-7-associated long QT syndrome (LQTS), a disorder of myocellular repolarization that predisposes affected persons to life-threatening ventricular tachyarrhythmia and sudden cardiac death (Curran et al., 1995; Keating et al., 2001). Currently, there are about 200 LQTS-associated mutations in hERG that have been reported. Approximately 1 in 5000-10,000 people is affected by LQTS-causing mutations in hERG and another K^+ channel gene, KCNQ1 (Modell and Lehmann, 2006).

Soon after the protein was expressed in *Xenopus* oocytes, hERG was found to encode the pore-forming subunit of the voltage gated K^+ channel that conducts the rapidly activating

delayed rectifier K^+ current (I_{Kr}) (Sanguinetti et al., 1995; Trudeau et al., 1995). I_{Kr} plays a critical role in cardiac repolarization. Reduction of I_{Kr} due to mutations in hERG or drug blockade of the channel causes LQTS and even sudden death (Haverkamp et al., 2000). Compared to LQTS caused by mutations in hERG (inherited LQTS), LQTS caused by drug block (acquired LQTS) is far more frequent and is a side effect of a variety of common medications such as some antiarrhythmic agents, antihistamines and antibiotics. In theory, a reduction of any voltage gated K^+ current that contributes to ventricular repolarization could cause LQTS. However, almost all of drugs that are known to cause LQTS preferentially block hERG channels (Mitcheson et al., 2000; Roden et al., 1996), and hERG blockade by different drugs represents a significant problem in drug safety. Thus, it is of great interest to understand the structural determinants for hERG channel function and drug-hERG channel interaction.

2. Role of hERG K^+ channels in the heart

hERG encodes a voltage gated K channel that is expressed in multiple tissues and cell types including neural (Warmke et al., 1994), smooth muscle (Farrelly et al., 2003), cardiac (Sanguinetti et al., 1995; Trudeau et al., 1995; Faravelli et al., 1996) and tumor cells (Chiesa et al., 1997; Smith et al., 2002). The role of hERG is best understood in regulation of cardiac function. As a member of voltage gated K^+ channels, hERG plays an important role in maintaining the cardiac action potential. Cardiac action potential was originally defined as the electrical events to initiate cardiac contraction. It's a rapid change in the membrane potential followed by a return to the resting membrane potential. The duration of the action potential usually parallels the duration of the cardiac

contraction. Action potentials are generated by voltage-dependent ion channels. The size and shape of action potential are determined by the population of the channels. The various phases of the cardiac action potential are associated with changes in the permeability of the cell membrane, mainly to potassium, sodium, and calcium ions. Under physiological conditions, the concentration of potassium ions inside a cardiac muscle cell is far greater than the concentration outside the cell. The reverse concentration gradient exists for sodium and calcium ions. Hence, K^+ tends to diffuse from the inside to the outside of the cell in the direction of the K^+ concentration gradient. However, many of the anions, such as proteins, inside the cell, are not free to diffuse out with the K^+. Therefore, the K^+ diffuses out of the cell and leaves the impermeant anions behind. The deficiency of cations then causes the interior of the cell to become electronegative which opposes positively charged potassium ion to flow the outside of the cell. Therefore, two opposing forces are involved in the movement of K^+ across the cell membrane. A chemical force based on the concentration gradient results in net outward diffusion of K^+. The counterforce is the electrical potential difference. When the two forces are equal, there is no net force on the K^+ ion. The electrical membrane potential at which there is no K^+ flow is called the potassium equilibrium potential (E_K) or reversal potential. For mammalian myocardial cells, the calculated value of E_K equals about -95 mV. As for sodium ions, the intracellular Na^+ concentration is much lower than the extracellular concentration. The sodium equilibrium potential, E_{Na}, is about 70 mV. This is to mean that at cell membrane potentials less than 70 mV, Na^+ tends to flow inside the cell from outside. At the resting membrane potential since Na^+ channels are not open, diffusion of Na^+ is very limited. On the other hand, since one type of K^+ channels are

open, diffusion of K^+ is optimized. The major portion of the resting membrane potential is a result of the diffusion of Na^+ and K^+ down their electrochemical potential gradients, with each ion tending to bring the membrane potential toward its own equilibrium potential. When the balance is reached, there is no net ion flow in the resting cell. This equilibrium potential for resting cell is called resting membrane potential (E_m). E_m is about -80 mV in myocytes. The relationship of E_K, E_{Na} and E_m is illustrated in scheme 1.

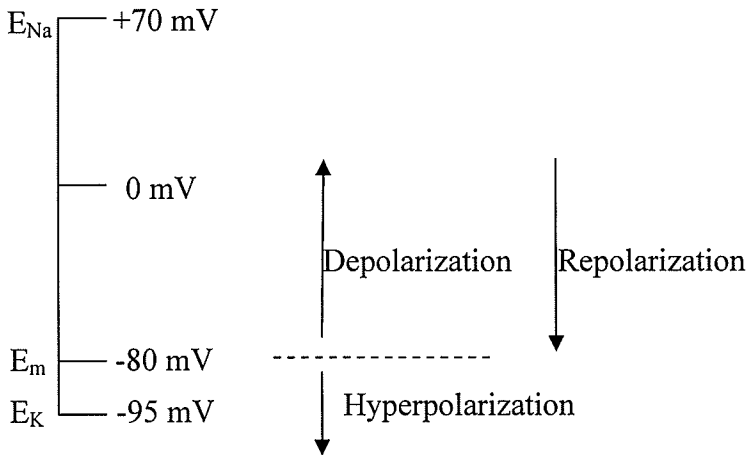

Scheme 1. The relationship of E_K, E_{Na} and E_m. The arrows indicate the directions of the membrane potential changes upon depolarization or repolarization.

Whereas ions are differently distributed across the cell membrane, only ions that membrane allows to permeate determine the membrane potential. When cell membrane is excited and Na^+ channels open, a large amount of Na^+ ions flowing into the cell would cause the membrane potential to increase from E_m (-80 mV) toward E_{Na} (more positive

potential). This change in potential is a depolarization because it decreases the potential difference, or polarization, across the membrane. Conversely, when K^+ channels are open, a large amount of K^+ ions flowing out of the cell would cause the membrane potential to decrease toward E_K. This change in potential is a repolarization which increases the polarization of the membrane. Any flux of K^+ takes place mainly through specific K^+ channels. Several types of K^+ channels exist in the cardiac cell membrane. The K^+ current conducted by these K^+ channels contributes to shaping the cardiac action potential including the transient outward current (I_{to}), the delayed rectifier repolarizing current consisting of the rapidly (I_{Kr} encoded by hERG) and slowly (I_{Ks} encoded by KvLQT1 + minK) activating components (Sanguinetti and Jurkiewicz, 1990a) and the inward rectifier I_{K1} current. These K^+ currents are encoded by different genes and flow through different types of K^+ channels. The sequential open of these distinct K^+ channels over different time frames represents a system to control and ensure the repolarization of the cell. For example, the class of K^+ channels that open first during action potential is rapidly activating and inactivating K^+ channels. This type of K^+ channels open quickly in response to the depolarization of the membrane potential and also close rapidly once the channels open even though the cell maintains the positive membrane potentials. In this case, the channel only allows a transient outward K^+ current (I_{to}) to flow out. This transient efflux of K^+ ions causes a brief period of early repolarization of the action potential. Then the delayed rectifying K^+ channels open, which conduct two different components of K^+ currents, the rapidly (I_{Kr} encoded by hERG) and slowly (I_{Ks} encoded by KvLQT1 + MinK) activating components. I_{Ks} occurs later than I_{Kr}, but lasts longer

than I_{Kr}. The properties of this type channels, especially hERG channels, will be discussed later.

There are five distinct phases (Phases 0 to 4, scheme 2) involved in the cardiac action potential. The rapid upstroke of the action potential caused by inward sodium current is designated phase 0. The upstroke is followed immediately by a brief period (a few milliseconds) of partial, early repolarization caused by the transient outward K^+ current (I_{to}) flowing through fast activating and inactivating K^+ channels. This brief repolarization is represented by a notch between the end of the upstroke and the beginning of the plateau. During the plateau phase (phase 2), the inward Ca^{2+} currents acts as the depolarizing force while the outward K^+ currents act as the repolarizing force. The balance between the inward and outward currents maintains the plateau phase which persists for about 0.2 seconds. The membrane then repolarizes (phase 3) to the resting membrane potential. The phase 3 repolarization starts when the efflux of K^+ begins to exceed the influx of Ca^{2+}. Repolarization develops more slowly than does depolarization (phase 0), which makes the cardiac muscle refractory to premature excitation. The I_{Kr} conducted by hERG channel is one of the most important component of phase 3 (scheme 2) (Sanguinetti et al., 1995; Trudeau et al., 1995). In ventricular myocytes, phase 4 represents the resting membrane potential until the next action potential.

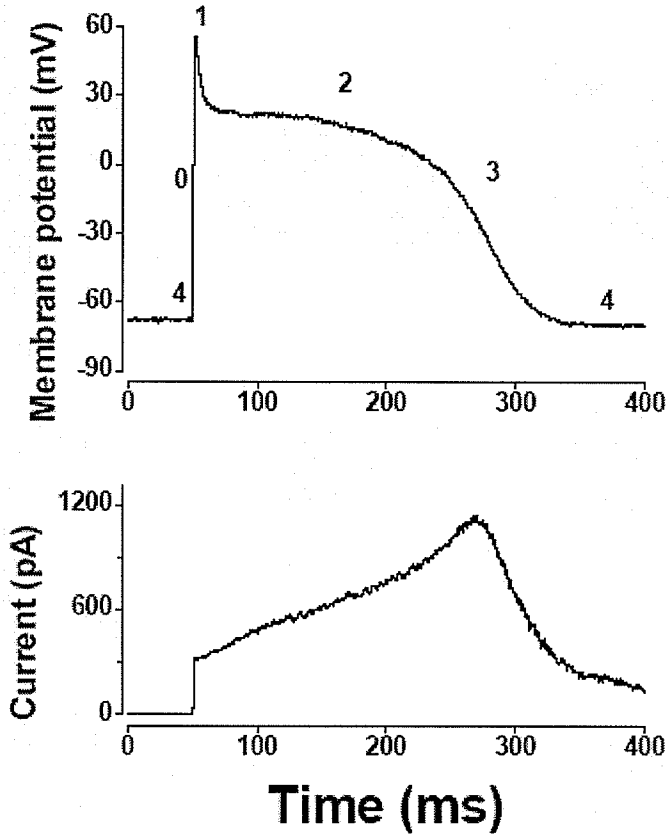

Scheme 2. The rapidly activating delayed rectifier K^+ current (I_{Kr}) during the ventricular action potential.

The upper panel shows the action potential profile, while the lower panel shows the corresponding I_{Kr} current.

HERG has unusual kinetics characterized by slow activation and deactivation, but rapid inactivation and recovery from inactivation (Sanguinetti et al., 1995; Trudeau et al., 1995; Zhou et al., 1998). At resting membrane potential (for example, -80 mV), hERG channels are closed. Depolarization more positive than -60 mV in phase 0 activates hERG channels to open state. However, the channel will also automatically close at a higher rate than channel opening at voltages > -20 mV. This channel closing process during the maintained depolarization is called inactivation. Thus, in the plateau phase when the membrane potential is above -20mV, hERG channels are inactivated, which reduces outward K^+ currents and contributes to the characteristic long plateau phase of the cardiac action potential. When the potential progressively decreases below -20 mV, hERG channels quickly recover from inactivation state to the open state, which induces a fast increase of conductance of hERG channels which effectively repolarizes the cell membrane to the resting level. Then hERG channels slowly close from the open state due to the membrane potential approaching to the resting level. This channel closing process is called deactivation which is slower than hERG recovery from inactivation and voltage-dependent.

3. Inherited LQTS caused by hERG mutations

Cardiac arrhythmias are one of the major causes of death in the developed world. They are most commonly associated with heart disease during, for example, a myocardial infarction or in hypertrophied and/or failing hearts. Arrhythmias are also characteristic of the relatively rare congenital long QT syndromes, which is an inherited condition associated with prolongation of the QT interval on the surface electrocardiogram. The

surface electrocardiogram is recorded by placing electrodes on the body surface. The relative magnitude and direction of each voltage deflection is dependent on the precise placement of the electrodes on the body. Typically, the first deflection (P wave) is upwards and reflects atrial depolarization. The second component usually consists of a small negative deflection (Q wave), followed by a large positive deflection (R wave) and a small negative deflection (S wave). The QRS complex reflects ventricular depolarization. The third major component is a broad positive deflection (T wave) that reflects ventricular repolarization. The QT interval is defined as the time interval between the onset of the QRS complex and the end of the T wave (scheme 3) and therefore, includes both the ventricular depolarization and repolarization intervals. Because of hERG's significant role in cardiac repolarization, reduction of hERG current could prolong the ventricular action potential. Since the QT interval reflects the duration of individual action potentials in cardiac myocytes, prolongation of the action potential duration will result in a prolonged QT interval. One of the criteria for diagnosing long QT syndrome is a QT >440ms. Mutations in hERG gene have been identified for congenital long QT syndrome, which is associated with an increased risk of an unusual life-threatening form of arrhythmia known as *torsade de pointes* (TdP). TdP is a distinctive polymorphic ventricular tachycardia characterized by QRS complexes of changing amplitude and contour that appear to twist about the isoelectric line. This arrythmia can be self-limiting or can degenerate into ventricular fibrillation, which will rapidly lead to death (Schwartz, 1997).

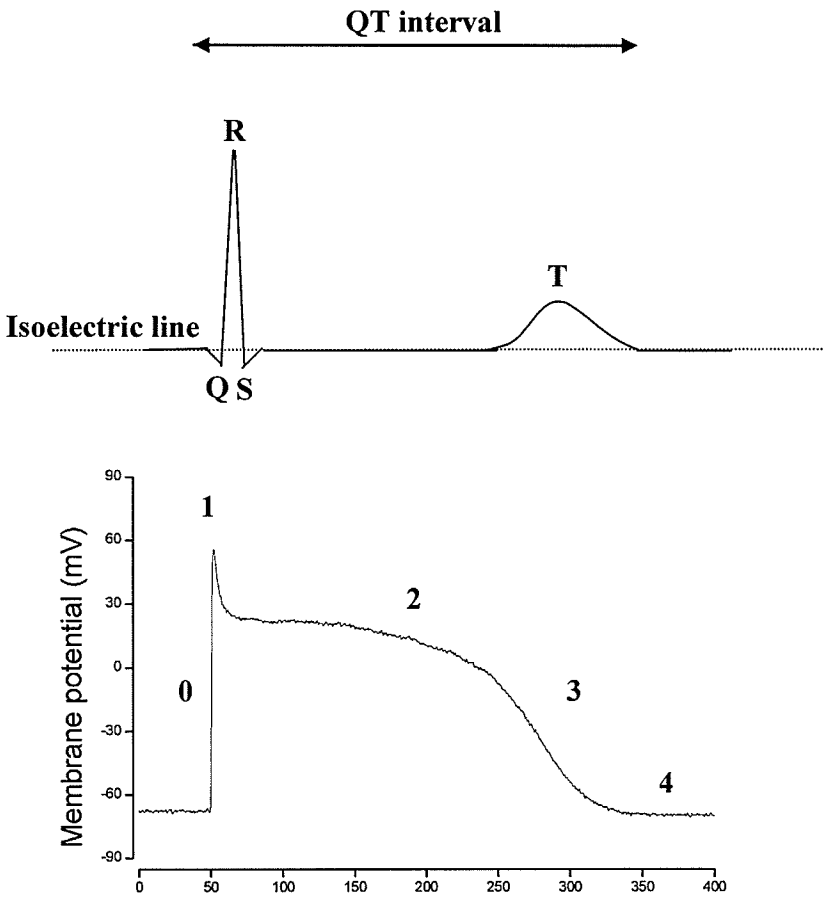

Scheme 3. Electrical gradients in the myocardium can be detected on the body surface electrocardiogram (ECG). Upper panel: An illustrative example of the measurement of the QT interval (from the beginning of the Q wave to the end of the T wave). Lower panel: Schematic representation of cellular electrical activity underlying the ECG.

In addition to hERG, mutations of other channel genes have also been identified for inherited LQTS. KCNQ1 (also known as KvLQT1) (Wang et al., 1996a) encodes the α-subunit of the K^+ channel that conducts the slowly activating delayed rectifier K^+ current,

I_{Ks}. Mink is the β- subunit associated with KCNQ1 to form functional channels mediating I_{Ks} (Barhanin et al., 1996; Sanguinetti et al., 1996b). Mutations in the Na^+ channel gene SCN5A can also result in inherited LQTS (Wang et al., 1995). Among all genes associated with the inherited LQTS, mutations in hERG account for 45%.

Most hERG mutations disrupt the proper folding of the subunits and trafficking of the channel to the cell surface membrane (Furutani et al., 1999; Delisle et al., 2004). Mutated and misfolded hERG proteins usually can not be transported to the cell surface membrane and are retained in the endoplasmic reticulum as the core–glycosylated premature form of the protein (Roden and Balser, 1999). These premature proteins are rapidly degraded by the ubiquitin – proteasome pathway (Gong et al., 2005). Some other mutations cause LQTS by altering hERG gating, such as accelerating inactivation (Nakajima et al., 1998), or causing dominant negative suppression when mutant and wild-type subunits coassemble (Sanguinetti et al., 1996a; Kagan et al., 2000). In summary, all of the hERG mutations cause inherited LQTS by reducing I_{Kr} current.

4. Acquired LQTS caused by drug-induced block of hERG channels.

While the congenital LQTS is relatively rare, acquired LQTS caused by a variety of common medications (Tristani-Firouzi et al., 2001) is far more frequent. It is interesting that nearly all known drugs that cause LQTS preferentially block the hERG channel (Roden et al., 1996; Mitcheson et al., 2000). However, the mechanisms of drug-hERG interactions are not well understood and are of significant interest for drug safety. Site-directed mutagenesis has identified residues Thr-623, Ser-624, and Val-625 in the pore

helix and aromatic residues Tyr-652 and Phe-656 in the S6 transmembrane segment of hERG subunits to be important molecular determinants for high-affinity drug binding to hERG channels (Lees-Miller et al., 2000; Perry et al., 2004). In addition to the structural determinant residues, the inactivation gating of hERG seems also important for high-affinity drug binding (Ficker et al., 1998; Zhang et al., 1999). For example, the structurally related EAG channel that has the tyrosine and phenylalanine residues equivalent to Tyr-652 and Phe-656 and has the residues equivalent to Thr-623, Ser-624, and Val-625 of hERG but does not inactivate, is not sensitive to the hERG blocker dofetilide. Sensitivity to block by dofetilide was introduced when the EAG channel was made capable of inactivating by mutations (Ficker et al., 2001). In addition, mutations that disrupt inactivation reduce the potency of blockade by various compounds (Ficker et al., 1998; Zhang et al., 1999). Recent studies, including ours, further suggested that it is the positioning of the aromatic residues in the S6 segment, not inactivation *per se*, that dictates the sensitivity of hERG to cisapride (Chen et al., 2002; Lin et al., 2005). This result is consistent with our recent study on cocaine block of hERG channels. We have found that the inactivation gating and cocaine block are not coupled (Guo et al., 2006).

In addition to direct block of hERG, some drugs have been recently identified to induce LQTS by disrupting hERG trafficking. It was reported that blockade of the ATPase activity of Hsp90 by geldanamycin resulted in the immature, core-glycosylated form hERG protein being retained in the endoplasmic reticulum (ER) (Ficker et al., 2003). It was also found that geldanamycin prolongs the action potential duration and reduces I_{Kr} without affecting other cardiac potassium currents such as I_{Ks} and I_{Kur}.

Pentamidine, a drug used to treat leishmaniasis and trypanosomiasis, can cause QT prolongation and *TdP*. It was found pentamidine disrupts hERG trafficking characterized by the absence of the fully mature protein on Western blot (Kuryshev et al., 2005).

5. The gating properties of the hERG channel

A structural model of hERG based on crystal structures of bacterial channels KcsA, KvAP and MthK (Doyle et al., 1998; Jiang et al., 2002b; Jiang et al., 2002a), indicates that hERG is formed by the coassembly of four identical subunits, each containing of six α helix transmembrane domains, S1-S6 (scheme 4). The S5, pore helix and S6 transmembrane domains compose the K^+-selective pore domain. The S1-S4 transmembrane domains comprise the voltage-sensing component of the channel. The S4 is by far the most important part of the voltage sensor, with several positively charged amino acids spaced three residues apart. Some of the basic residues in S4 also interact with the few acidic residues located in the S2 and S3 transmenbrane domains. The hERG protein is composed of 1159 amino acids with both extended N- and C- termini in the intracellular side. Different from most other voltage-gated K^+ channels, hERG activates slowly and inactivates rapidly. The regions thought to be important for slow activation and deactivation include the N-terminal PAS domain (Scheme 4), the S4-S5 linker and the end of the S6 domain. The structural basis for rapid inactivation is unknown, but it is presumed to be somewhat similar to the C-type inactivation, involving residues interactions between S5 and the pore loop.

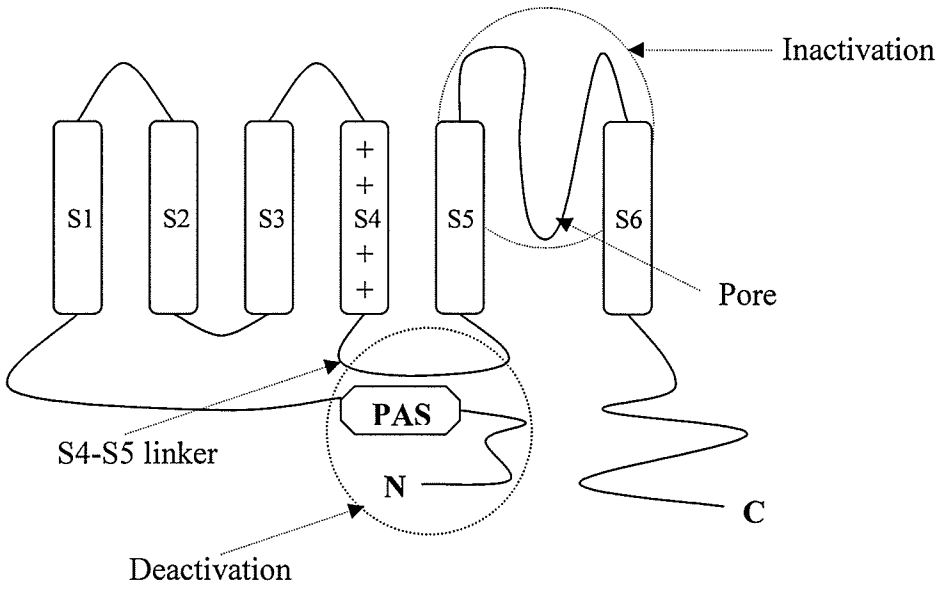

Scheme 4. Diagram of a single hERG subunit containing six α-helical transmembrane domains, S1–S6.

Previous studies on K^+ channels suggested the existence of an intracellular activation gate whose opening allows the entry of ions or drugs into the inner channel pore (Armstrong, 1971). Similarly, hERG possesses an intracellular gate which opens in response to the outward movement of the voltage sensor, S4 transmembrane domain (Stefani et al., 1994; Bezanilla et al., 1994; Stühmer et al., 1991). Based on the crystal structure of the MthK channel, the open K^+ channel model, and KcsA channel, the closed K^+ channel model, the activation gate of hERG channels is formed by the S4-S5 linker and the C-terminal portions of the S6 domain which crisscross to form a narrow aperture near the cytoplasmic interface (Holmgren et al., 1998). Splaying of the S6 helices at a conserved

glycine (G648 in hERG) which serves as a hinge point leads to the channel opening and the aperture expending, and therefore the ions can permeate through the channel (Jiang et al., 2002a; Jiang et al., 2002b) (scheme 5). Most recent studies on chimerical constructs of hERG and EAG channels confirmed that a direct interaction exists between the S4-S5 linker and the activation gate in the process of channel opening which is also coupled with voltage sensing (Ferrer et al., 2006).

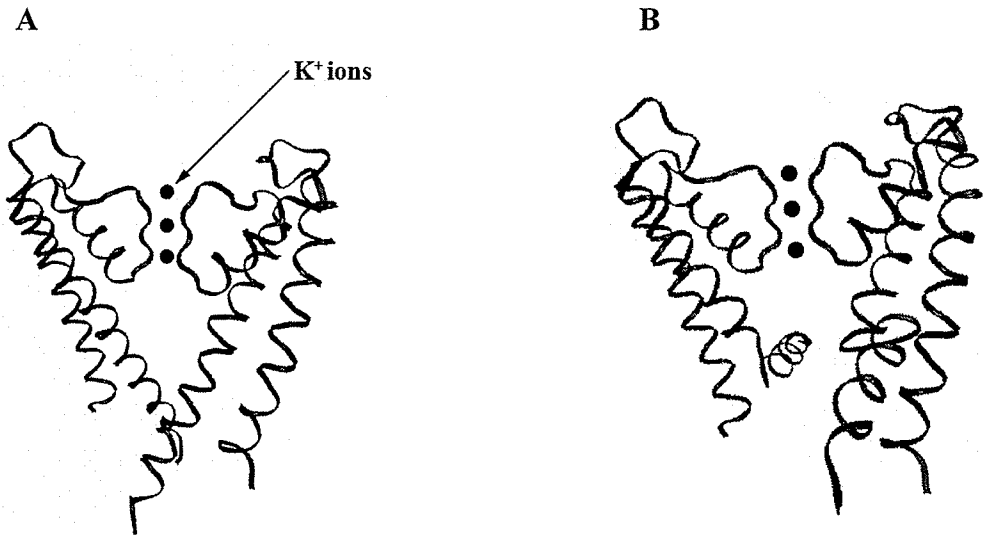

Scheme 5. Crystal structures of voltage-gated K^+ channels

A, Structure of a KcsA K channel crystallized in the closed state. Only two of the four subunits are shown. Black spheres are K^+ ions located within the selectivity filter. B, Structure of the pore domain of a voltage-gated K^+ channel crystallized in the open state.

The slow deactivation of the hERG channel contributes to the final repolarization of the cardiac action potential. Some LQT2-associated mutations reduce repolarization currents via accelerating channel deactivation and therefore prolonging the action potential duration (Chen et al., 1999b). It was found that the NH_2-terminus of hERG plays a key role in the deactivation process. Deletion of the first 354 amino acids (Wang et al., 1998; Spector et al., 1996) or the first 373 amino acids (Schönherr et al., 1996) in the NH_2-terminus causes a ten-fold acceleration of channel deactivation. It is revealed that the hERG NH_2-terminus contains a basic helix-loop-helix "Per-Arnt-Sim" (PAS) domain which is the key component of some sensing and signal transduction proteins (Morais Cabral et al., 1998). The PAS domain in hERG might interact with an accessory protein or other regions of the channel, and stabilize NH_2-terminus binding to the activation gate. However, there is no direct evidence to prove the above proposal and the role of the PAS domain in hERG remains unclear.

The most important feature of the hERG channel is the fast, voltage-dependent inactivation of the channel (Sanguinetti et al., 1995; Trudeau et al., 1995). As mentioned previously, the fast inactivation limits outward current through the channel at positive voltages and helps maintain the action potential plateau phase. However, the molecular mechanism underlying the inactivation gate is not well understood.

There are two types of inactivation in Kv channels: fast N-type inactivation and slow C-type inactivation. The molecular mechanism of N-type inactivation was first found in *Shaker* channels and a "ball-and-chain" model was proposed (Hoshi et al., 1990; Zagotta

et al., 1990). It suggests that a short segment in the NH_2 terminus of the channel protein binds and occludes the intracellular activation gate (Hoshi et al., 1990; Zagotta et al., 1990; Lopez et al., 1994; Isacoff et al., 1991; Holmgren et al., 1996). The N-type inactivation occurs in milliseconds and can be removed by NH_2-terminal deletion (Hoshi et al., 1990; Zagotta et al., 1990). Three properties distinguish N-type inactivation from other type of inactivation. First, the rate of development of N-type inactivation is affected by intracellular but not extracellular drug binding (Choi et al., 1991; Demo and Yellen, 1991). Second, N-type inactivation is not affected by positive potentials (Zagotta and Aldrich, 1990). Third, N-type inactivation is not sensitive to point mutations at the outer mouth of the channel pore and the outer region of S6 helix (Hoshi et al., 1990; Lopez-Barneo et al., 1993; Rasmusson et al., 1995).

In addition to N-type inactivation, there is another type of inactivation identified in *Shaker* K^+ channels, called C-type inactivation. C-type inactivation occurs due to the constriction of the outer mouth of the channel pore and involves multiple conformational changes (Olcese et al., 1997; Yang et al., 1997b; Loots et al., 1998; Kiss et al., 1999; Wang et al., 2001). C-type inactivation occurs much slower than N-type inactivation and usually is referred to as slow inactivation. C-type inactivation of K^+ channels represents a general mechanism of a broad number of channels including Na^+ channels (Balser et al., 1996; Wang and Wang, 1997) and Ca^{2+} channels (Zhang et al., 1994). C-type inactivation of K^+ channels exhibits several properties. First, C-type inactivation is not affected by mutations or deletions of the NH_2 terminus (Hoshi et al., 1990). Second, C-type inactivation exhibits a slow developmental rate by elevating the extracellular K^+

(Lopez-Barneo et al., 1993). Third, C-type inactivation is sensitive to the external but not internal TEA^+ block (Choi et al., 1991). Fourth, C-type inactivation is sensitive to point mutations at the external mouth of the channel pore and the outer region of S6 (Lopez-Barneo et al., 1993). Fifth, similar to N-type inactivation, C-type inactivation is not voltage dependent at positive potentials (Hoshi et al., 1990; Rasmusson et al., 1995).

The inactivation of hERG channels resembles the C-type inactivation of *Shaker* K^+ channels in its sensitivity to extracellular K^+ concentration and TEA^+, and to mutations in the P-loop (Hoshi et al., 1991; Smith et al., 1996; Schönherr et al., 1996; Fan et al., 1999). However, hERG inactivation also shows several unique properties that differ it from C-type inactivation of *Shaker* K^+ channels. The onset of *Shaker* C-type inactivation is very slow and is not obviously voltage dependent (Rasmusson et al., 1998). In contrast, onset of inactivation of hERG is much more rapid and strongly voltage-dependent (Smith et al., 1996; Spector et al., 1996). The difference between hERG and *Shaker* inactivation may be due to the fact that hERG has a more flexible pore. There are 43 amino acids in the hERG S5-P linker whereas there are 14 to 18 amino acids in the corresponding region of most other Kv channels (Dun et al., 1999). In addition, the *Shaker* sequence has double tryptophan residues (WW) at the N-terminal end of the pore-loop, and a tyrosine residue (Y) in the "signature motif" (GYG) at the C-terminal end. According to the crystal structure of KcsA, hydrogen bonds can be formed in the 3-dimensional structure around the outer mouth between the nitrogens of "WW" and the hydroxyl group of "Y" of the four subunits. These hydrogen bonds serve as "molecular springs", that pull the pore wall radially outward to hold the outer mouth open at its proper diameter (Doyle et al., 1998). The corresponding tryptophan and tyrosine residues are missing in hERG. The

absence of hydrogen bonds and a longer S5-P linker segment may lead to a more flexible pore (Tseng, 2001). In terms of the voltage dependence of hERG inactivation, a recent model presented by Berneche and Roux (Berneche et al., 2005) may give a potential explanation. According to the model, there is a modest rearrangement that leads to a nonconducting conformational state of the selectivity filter, which is then effectively acting as a gate. This structural rearrangement involves only one of the four subunits at a time, breaking the 4-fold symmetry of the channel. The first step, which initiates the conformational transition toward the nonconducting state, is very sensitive to the configurations of the ion occupying the selectivity filter. Membrane depolarization (positive voltage shift) favors a state in which the transition can take place, and membrane polarization (negative voltage shift) favors a state which prevents the transition.

Although considerable effort has been directed toward defining the structural basis of the inactivation gate, the molecular mechanism underlying the unique hERG inactivation remains unclear partially because of the lack of direct way to monitor the inactivation gate since it is non-permeable to K^+ ions. Our most recent studies provide a direct way to investigate the hERG inactivation process by studying Na^+ currents in hERG channels (Gang and Zhang, 2006). Our data suggested that the hERG channels undergo at least two distinct inactivation steps. The initial, less stable P-type inactivated state is quickly reached upon depolarization, and is followed by a slow entry into the more stable 'C-type' inactivated state. We use "P-type inactivation" to mean that a limited conformational change in the channel pore is sufficient to block K^+ permeation. We used

"C-type inactivation" to indicate that hERG channels can experience more substantial conformational changes which cause immobilization of the channel charge seen typically in C-type inactivation of *Shaker* channels. The P-type inactivated state is the Na^+ permeating state, while the 'C-type' inactivated state is nonconducting.

III. STATEMENTS OF HYPOTHESIS

We propose that Na^+ ions can permeate inactivated hERG channels. This way, we will have a direct means to "see" the inactivated channels. This new approach will facilitate studies of hERG inactivation mechanisms and drug - channel interactions. We have recorded a robust Na^+ current through hERG channels by using the whole cell patch clamp with an internal solution containing 135 mM Na^+ and an external solution containing 135 mM NMG^+. We used two approaches to investigate the state that Na^+ permeates through: analysis of the current kinetics and mutations. Kinetic analyses of the hERG Na^+ and K^+ currents indicate that the channel experiences at least two states during the inactivation process, an initial fast, less stable state followed by a slow, more stable state. The Na^+ current reflects Na^+ ions permeating through the fast inactivated state but not through the slow inactivated state. Thus the hERG Na^+ current displayed a slow inactivation as the channels travel from the less stable, fast inactivated state into the more stable, slow inactivated state.

In the second approach, mutations were constructed to accelerate or remove hERG inactivation. We found that T623A, F627Y and S641A significantly accelerated hERG inactivation to such an extent that no significant K^+ current could be detected in the physiological solutions (K^+ ions can not permeate through inactivated channels.). However, robust Na^+ currents were recorded. These results indicate that Na^+ permeation state is the inactivated state. Consistent with this notion, we found that Na^+ does not permeate through the inactivation deficient mutant channel, S631A.

Our study represents the first study that has characterized Na^+ permeation through hERG channels. The resultant paper on this project has been published in *Journal of General Physiology (Gang and Zhang, J. Gen. Physiol.* 128:55-71, 2006). The reason why such an important issue has never been previously reported are not known, but we further found that external Na^+ potently blocks hERG Na^+ current. Thus, no Na^+ current could be recorded in external solutions containing Na^+. We found that point mutations in the pore region of the channel, S624A, F627Y and S641A, abolish the inhibitory effects of the external Na^+ ions on the hERG Na^+ current.

IV. MATERIALS and METHODS

1. Materials

hERG cDNA in pcDNA3 was obtained from Dr. Gail A. Robertson (University of Wisconsin-Madison, Madison, WI, USA). The HEK 293 cell line was purchased from American Type Culture Collection (Manassas, VA, USA). The HEK 293 cell line stably expressing hERG channels was a gift from Dr. Craig January (University of Wisconsin-Madison, Madison, WI, USA). Minimum essential medium (MEM), Fetal Bovine Serum, 0.05% Trypsin-EDTA and Lipofectamine 2000 were purchased from Invitrogen Life Technologies (Carlsbad, CA, USA). G418 was from SIGMA-ALDRICH (St. Louis, MO, USA). All the enzymes used were purchased from New England Biolabs (Beverly, MA, USA). 1 kb DNA ladder, 10 mM dNTP Mix (PCR grade), Zero Blunt Kit and Subcloning efficiency DH5α competent cells were from Invitrogen Life Technologies (Carlsbad, CA, USA). Thin-walled borosilicate glass was from World Precision Instruments (Sarasota, FL, USA). All other chemicals were purchased from SIGMA-ALDRICH (St. Louis, MO, USA).

2. Methods

2.1. Site-directed mutagenesis

An expression plasmid of wild type (WT) hERG was constructed by inserting the full length coding region of the hERG gene (3.9 kb) into the *BamHI/ EcoRI* sites of the pcDNA3 vector as shown in scheme 6, which contains two suitable unique enzyme sites (*BstEII and SbfI*) covering the S5-P loop region we are interested in (referred to as region of interest in the scheme). As shown in scheme 7, point mutations (BmS, ▲) of hERG were generated by PCR using the splice overlap extension technique (Ho et al., 1989). The forward and reverse flanking primers (P1 and P4) were designed to cover two unique restriction sites (*BstE*II at nucleotide 2038 and *Sbf*I at nucleotide 3093). The first round of PCRs was performed using the forward flanking primer (P1)-reverse mutant primer (Pmr), and the reverse flanking primer (P4)-forward mutant primer (Pmf), respectively. Primers used for amplification were synthesized as shown in table 1. In the first round of PCRs, the total reaction volume was 50 μl, including 50 pmol of each primer, 70 ng of WT hERG cDNA, 0.2 mM dNTP and 0.125 units of Vent DNA polymerase. Temperatures used for PCR were as follows: 95°C for 120 s for 1 cycle; denaturation at 94°C for 60 s, annealing at 68°C for 60 s and extension at 72°C for 60 s for 30 cycles; and final extension at 72°C for 10 min. The resulting two PCR products were then used as templates and amplified by flanking primers (P1 and P4) in a second round of PCR. The final PCR product was cloned into the Zero Blunt Vector. A 1055 bp fragment containing the point mutation was excised by digestion with *BstE*II and *Sbf*I, and then subcloned into the pcDNA3 vector containing the WT hERG at the same sites (scheme

8). All mutations were verified using a high-throughput 48 capillary ABI 3730 sequencer (UCDNA Services, University of Calgary, Calgary, AB, Canada).

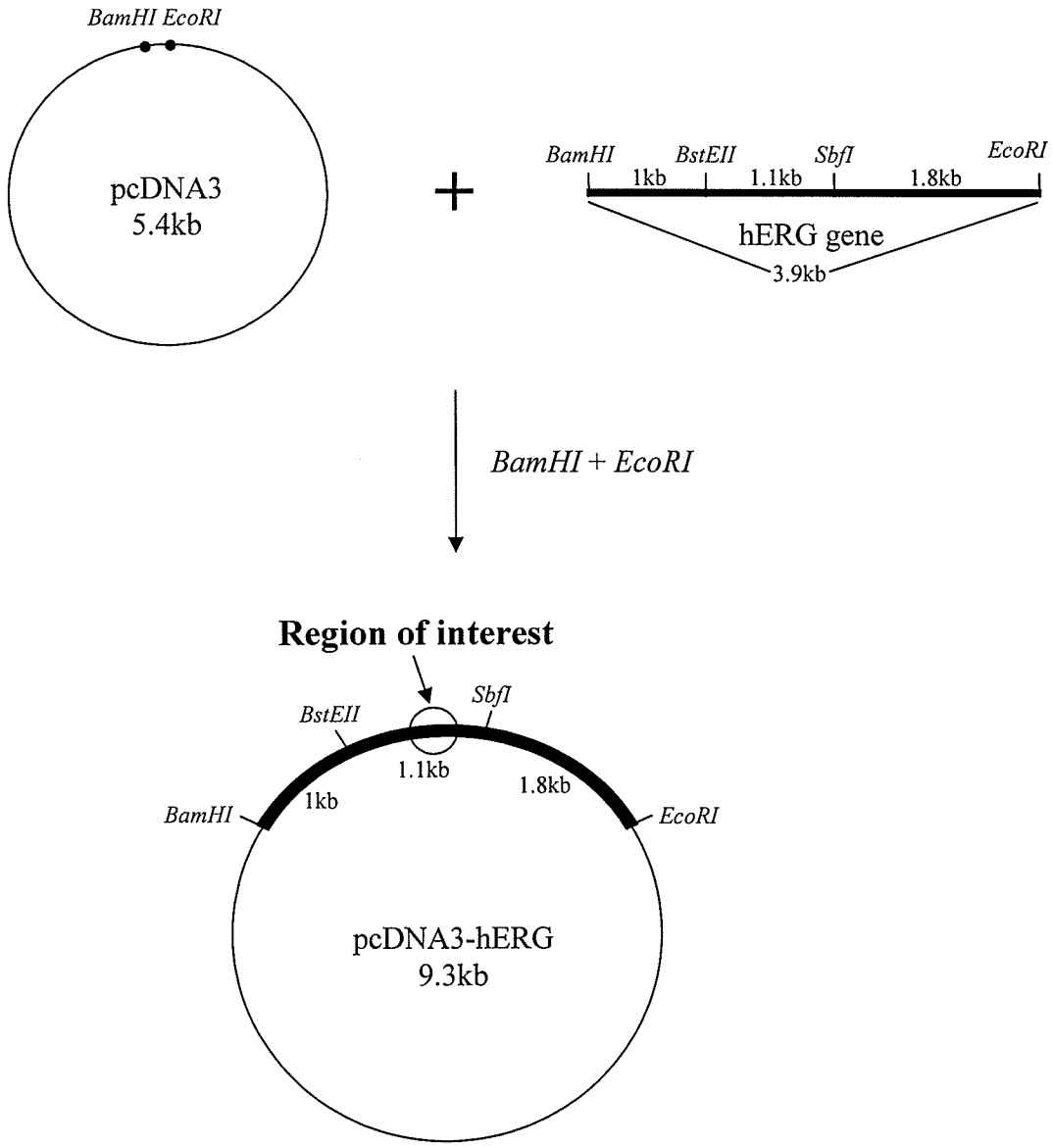

Scheme 6. Expression plasmid of wild type hERG

hERG gene was cloned into the *BamHI / EcoRI* sites of pcDNA3 vector. The S5-P loop region is referred to as region of interest which is covered by two unique enzyme sites, *BstEII* and *SbfI* .

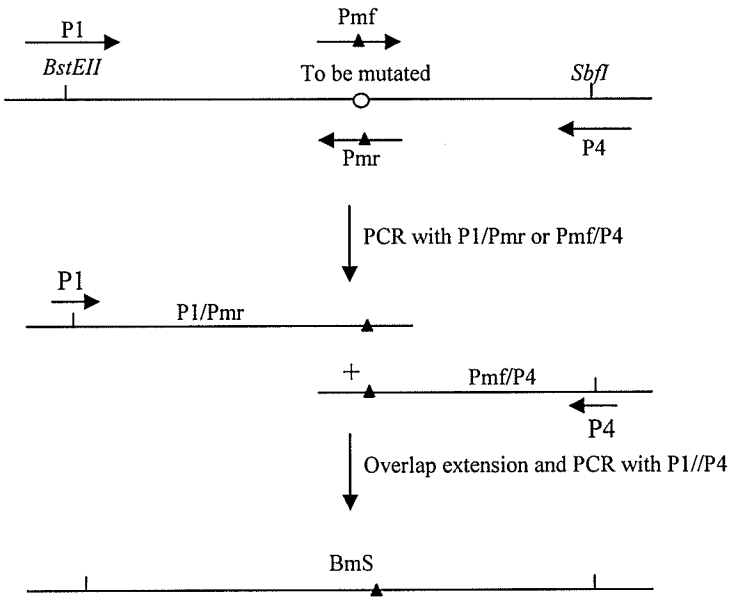

Scheme 7. Mutation PCR by overlap extension to introduce point mutation

The first round of PCRs was performed using two pairs of primers, P1and Pmr, Pmf and P4. The resulting two PCR products were then used as templates and amplified by P1 and P4 in a second round PCR. The final PCR product containing the desirable mutation (BmS, ▲) was obtained.

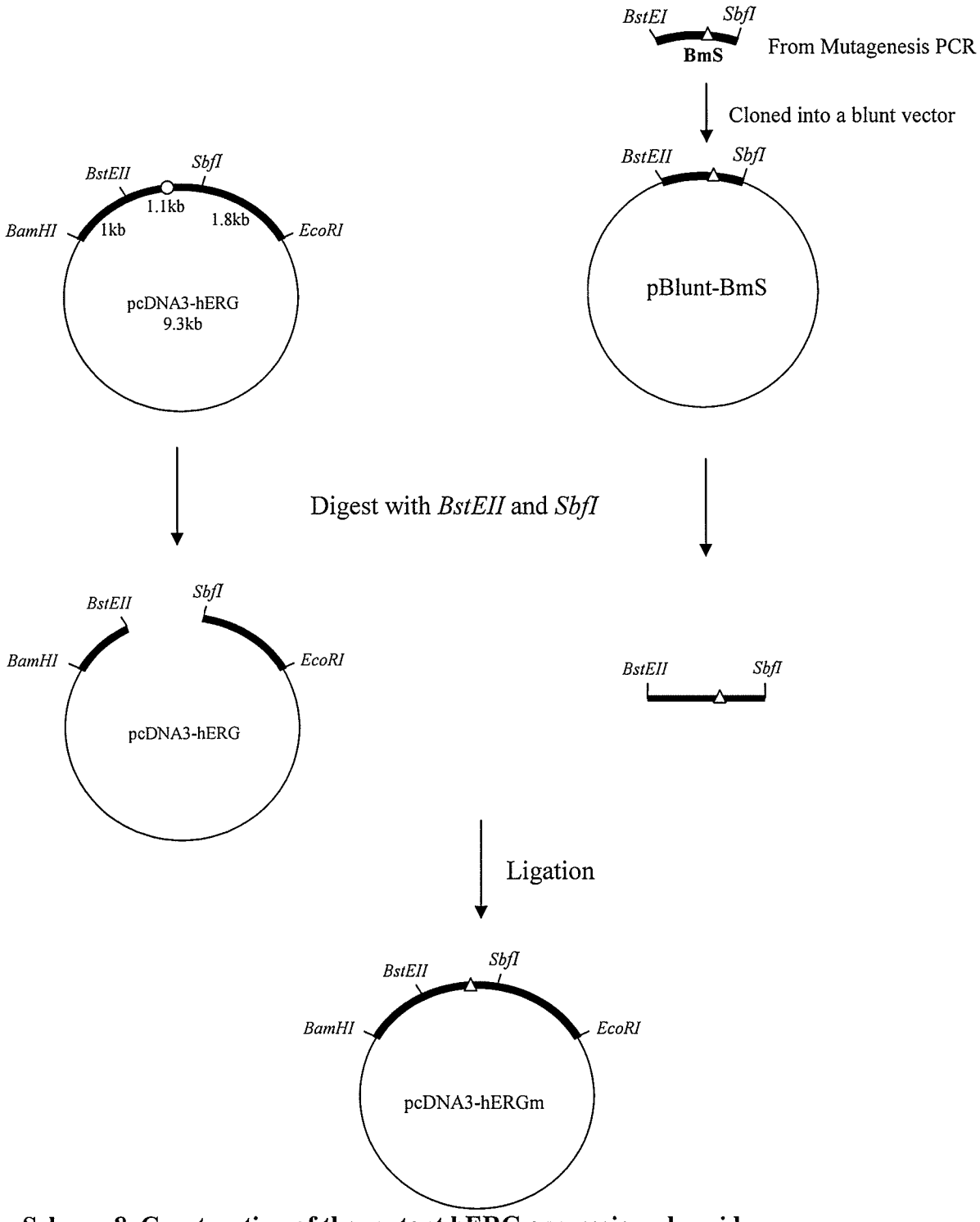

Scheme 8. Construction of the mutant hERG expression plasmid

The final PCR product from mutagenesis PCR was cloned into the blunt vector and the fragment was excised by digestion with *BstEII* and *SbfI*. The fragment then was cloned into the pcDNA3 vector containing the WT hERG at the same sites.

Table 1

Primers used for PCR reactions

Mutant nucleotides are underlined.

Primers		Sequence
Flanking	**Forward (P1)**	CCCACAATGTCACTGAGAAGGTCACCCAGG
	Reverse (P4)	GCAGTGAGCGGTTCAGGTGCAGGCAGATGTC
T623A	**Forward**	ACCTTCAGCAGCCTCGCCAGTGTGGGCTTC
	Reverse	GAAGCCCACACTGGCGAGGCTGCTGAA
S624A	**Forward**	ACCTTCAGCAGCCTCACCGCTGTGGGCTTCGGCAA CGTCT
	Reverse	AGACGTTGCCGAAGCCCACAGCGGTGAGGCTGCTG AAGGT
F627Y	**Forward**	CACCAGTGTGGGCTACGGCAACGTCTCTCCC
	Reverse	GGGAGAGACGTTGCCGTAGCCCACACTGGTG
S641A	**Forward**	TCAGAGAAGATCTTCGCCATCTGCGTCATG
	Reverse	GAGCATGACGCAGATGGCGAAGATCTTCTCTGA

2.2. Transient expression of hERG mutant channels in HEK 293 cells

HEK 293 cells were seeded at 5×10^5 cells/60-mm diameter dish. The cells were transiently transfected using 10 μl Lipofectamine with 4 μg hERG mutant expression plasmid. After 24-48 h, 30-80% of cells expressed channels. Non-transfected HEK 293 cells contain a small-amplitude background K^+ current that is usually less than 100 pA upon a depolarizing pulse to 50 mV. Thus, the effects of overlapping endogenous currents of HEK 293 cells on the expressed current are minimal. The HEK 293 cell line stably expressing hERG channels obtained from Dr. Craig January was also used. In this cell line, the hERG cDNA (Trudeau et al., 1995) was subcloned into *Bam*HI/*Eco*RI sites of the pcDNA3 vector. The stably transfected cells were cultured in MEM supplemented with 10% fetal bovine serum and contained 400 μg/ml G418 to select for transfected cells. For electrophysiological study, the cells were harvested from the culture dish by trypsinization, and stored in standard MEM medium at room temperature. Cells were studied within 8 h of harvest.

2.3. Patch clamp recording

The whole cell patch clamp method was used. The pipette solution contained (in mM) 135 NaCl, 5 EGTA, 1 $MgCl_2$, 10 HEPES, and was adjusted to pH 7.2 with NaOH. The bath solution contained (in mM) 10 HEPES, 10 glucose, 1 $MgCl_2$, 2 $CaCl_2$, 135 NMG^+, and was adjusted to pH 7.4 with HCl. For recordings in the presence of different external K^+ or Na^+ concentrations, the concentration of NMG^+ was proportionally reduced as the K^+ or Na^+ concentration was elevated to maintain a constant osmolarity, and the pH was adjusted to 7.4 with the appropriate hydroxide solution. Throughout the text the

subscripts *i* and *o* denote intra- and extra-cellular ion concentrations, respectively.

Aliquots of cells were allowed to settle on the bottom of a <0.5 mL cell bath mounted on an inverted microscope (TE2000, Nikon, Tokyo, Japan). Cells were superfused with specific bath solutions. The bath solution was constantly flowing through the chamber and the solution was changed by switching the perfusates at the inlet of the chamber, with complete bath solution change taking 10 s. Patch electrodes were fabricated using thin-walled borosilicate glass. The pipettes had inner diameters of ~1.5 μm and resistances of ~2 MΩ when filled with pipette solutions. An Axopatch 200B amplifier was used to record membrane currents. Computer software (pCLAMP9, Axon Instruments, Foster City, CA) was used to generate voltage clamp protocols, acquire data, and analyze current signals. Data were filtered at 5-10 kHz and sampled at 20-50 kHz for all protocols. Typically, 80% series resistance (R_s) compensation was used and leak subtraction was not performed. Conductance/voltage data were fitted to a single Boltzmann function, $y = 1 / (1+\mathrm{Exp}((V_{1/2}-V)/k))$, where y is the current normalized with respect to the maximal tail current, $V_{1/2}$ is the half-activation potential or mid-point of the activation curve, V is the voltage that activates the channels and k is the slope factor in mV, reflecting the steepness of the voltage dependence of gating. Curve fitting was done using multiple non-linear least squares regression analysis. Concentration effects of external Na^+ (Na^+_o) on the WT Na^+ current were quantified by fitting data to the Hill equation ($I_{Na}/I_{control} = 1/[1+(D/IC_{50})^H]$, where D is the Na^+_o concentration, IC_{50} is the Na^+_o concentration for 50% block, and H is the Hill coefficient of the results. Data are given as mean ± S.E.M. Clampfit (Axon Instruments) and Origin (OriginLab, Northampton, MA) were used for data analysis. All experiments were performed at room temperature (23 ± 1°C).

V. RESULTS

1. Na^+ permeation through hERG K^+ channels

Under conditions with an intracellular solution containing 135 mM Na^+ and a bath solution containing 135 mM NMG^+ without K^+ or Na^+, we have consistently recorded robust Na^+ currents in hERG-expressing HEK 293 cells. The protocol in Fig. 1A above the current traces was used to record Na^+ currents. Na^+ currents were activated by 4-s depolarizing pulses from a holding potential of -80 mV (resting membrane potential at which the channels are closed) to voltages between -70 and 70 mV in 10 mV increments. Upon depolarization, the channel is activated to open state. However, the open channels are quickly closed when the voltages are more positive than -20 mV. This process is called inactivation. Moreover, the stronger the depolarization, the more the channels are inactivated. This kind of inactivation is called voltage-dependent inactivation, which is unique to hERG channels. Thus, hERG K^+ currents get smaller when a bigger driving force is applied since bigger driving forces inactivated more channels and inactivated channels are K^+ impermeable. In contrast to the hERG K^+ current, the hERG Na^+ current increased in amplitude as the depolarizing voltage increased (Fig. 1A), which means that the more inactivated channels were available, the bigger the Na^+ current could be recorded. This result indicated that Na^+ may permeate through inactivated hERG channels. The Na^+ current was also sensitive to specific hERG blockers. As shown in Fig. 1B, the current was completely blocked by 1 μM astemizole (n = 5). The current was also sensitive to the methanesulfonanilide drug E-4031 (data not shown). In the non-transfected HEK 293 cells, no Na^+ current could be detected using a similar protocol

(Fig. 1C, n = 6). Contamination of Cl^- current was ruled out because the Na^+ current in hERG-HEK cells was not affected by the bath application of 100 μM DIDS, a specific Cl^- channel blocker. As well, changing Cl^- concentration by non-permeable glutamic substitution had no effect on the current. The Na^+ current was essentially the same when a pipette solution containing 135 mM Na-Glutamate instead of 135 NaCl was used (n = 4, data not shown). These results indicate that the Na^+ current reflects Na^+ permeation through hERG channels. Fig. 1D shows the current-voltage (I-V) relationships of the hERG Na^+ current amplitudes at peak (▲) and at the end of depolarizing steps (●) in 13 cells. Notably, the I-V relationships of the hERG Na^+ current are nearly ohmic (the higher the voltage, the larger the current), which are different from the inward rectification of the I-V relationships of the hERG K^+ current.

To further address whether the Na^+ permeating hERG channels are K^+ selective, we studied the effects of external K^+ (K^+_o) on the Na^+ current. K^+_o inhibits the outward Na^+ current with a K_D of 0.61 ± 0.08 mM (n = 7, Fig. 2), which means that 0.61 mM K^+_o can block half of the maximum outward Na^+ currents. Upon repolarization, the inward K^+ tail current appears and this inward current was completely abolished by 100 nM E-4031. These results indicate that hERG channels were intact and not "defunct" when Na^+ permeates since the channel still displayed K^+ selectivity and sensitivity to the specific hERG channel blocker (Almers and Armstrong, 1980; Melishchuk et al., 1998).

2. Electrophysiological properties of hERG Na^+ current

2.1. hERG Na^+ current activation and deactivation

To characterize hERG Na^+ current, we examined the time courses of current activation, deactivation, onset of inactivation and recovery from inactivation. The time courses of the current activation are apparently sigmoidal (Fig. 3A), which referred to the S-shape of the initial part of the current upon the depolarization. The initial sigmoidal component is ignored and a single exponential is fit to the remaining major portion of the current to obtain activation time constants (τ_{act}) at various voltages. The voltage dependence of the τ_{act} of the Na^+ current is summarized in Fig. 3D (▲, n = 13). These data indicated that the higher the voltage, the faster the current reached its peak.

Due to the extremely small tail current at negative voltages, deactivation properties of the hERG Na^+ current were studied using a three-pulse protocol as shown in Fig. 3B. In brief, deactivation refers to the channel close from the open state upon repolarization steps. From the holding potential of –80 mV, a depolarization to 70 mV for 250 ms (P1 pulse) was used to maximally activate the channels (to induce the peak amplitude). The cells were then repolarized to test potentials for various durations (P2 pulse) for channels to deactivate. The cell membrane was then depolarized to 70 mV again for 200 ms (P3 pulse) to monitor the instantaneous current amplitudes which represent the proportion of not-yet-deactivated channels during P2. The instantaneous current amplitudes upon P3 are plotted against the duration of P2 at -60, -80 and -100 mV (Fig. 3C). As the P2 prolongs, instantaneous current upon the P3 decreases (dotted line in Fig. 3B), reflecting the channel deactivation (channel closes upon repolarization) during various durations P2. The data points were fitted to a double exponential function, and the deactivation time constants (τ_{deact}) were obtained. The voltage dependence of τ_{deact} of the hERG Na^+

current is shown in Fig. 3D (▼, ●; n = 7). These data indicated that the lower the voltage, the faster the channel deactivated.

2.2. Inactivation of hERG Na^+ current

During sustained depolarizations, the hERG Na^+ current displayed a decay phase which may represent a slow inactivation since the channel's conductance reduced even though the activation voltage was maintained (Fig. 1A). To examine the voltage dependence of the hERG Na^+ current inactivation, a depolarizing step to 70 mV for 250 ms was used to induce the peak Na^+ current. The cells were then clamped to various voltages for 4 s to record the time course of the current decay which was fitted to a single exponential function (Fig. 4A). This current decay indicated that partial channels were inactivated upon depolarization steps which resulted in the decrease of the hERG channel conductance and reduction of currents. The time constants of the hERG Na^+ current inactivation (τ_{inact}) were plotted against the test voltages (Fig. 4B). Two features of Na^+ current inactivation are prominent; first, in contrast to the inactivation of hERG K^+ currents, the inactivation of hERG Na^+ currents is only weakly voltage dependent. Second, the τ_{inact} is nearly 1000-fold slower than that of the hERG K^+ current (n = 9).

Inactivation of the hERG K^+ current is very fast (time constant in millisecond ranges) and strongly voltage-dependent, leading to the characteristic inward rectification of the current-voltage relationships (Sanguinetti et al., 1995; Trudeau et al., 1995). In other words, hERG channels are inactivated when the membrane potential is above -20 mV. Stronger depolarizations more than -20 mV inactivate larger population of hERG

channels which results in the decrease of the K^+ currents since K^+ ions can not permeate through inactivated channels. This kind of current-voltage relationship of the hERG K^+ current is termed inward rectification. However, stronger depolarizing steps evoke larger outward hERG Na^+ currents with a slow decay (Fig. 1A & D). One of the explanations for this result is that the hERG Na^+ current represents Na^+ permeating through the inactivated hERG channels since the outward Na^+ currents became larger when more hERG channels were inactivated upon depolarization steps. Because we have also found that the Na^+ current slowly inactivates during the prolonged depolarizations (Fig. 4A & B), which mimics the typical C-type inactivation in *Shaker*, we propose that inactivation of the hERG channel involves at least two steps, the fast entry into the less stable, P-type inactivated state, and the slow entry into the more stable 'C-type' inactivated state. We propose that Na^+ permeates through the fast inactivated state (P-type) but not through either open state or 'C-type' inactivated state. Since P-type inactivation of the hERG channel occurs faster than channel opening, activation of the Na^+ current reflects transition from the closed state to the P-type inactivated state through the open state. We believe that the Na^+ current decay during depolarizations reflects the entry of the P-type inactivated channels into the 'C-type' inactivated state.

The notion that Na^+ permeates through the P-type inactivated state but not the open state is supported by the data shown in Fig. 4. Careful inspection of the current traces in Fig. 4A indicated that a fast decay of the Na^+ current immediately upon voltage changes from the initial depolarization of 70 mV. The portion of the Na^+ current traces during the 70 mV-depolarization and immediately upon voltage changes are expanded in Fig. 4C. The

fast decay of the Na^+ currents upon test pulses (Fig. 4C) was fitted to a single exponential function and the time constants were plotted against the test voltages (Fig. 4D, n = 6). We believe that the fast decay of Na^+ currents represents the recovery of P-type inactivated channels (Na^+ permeable) to the "open" state which is Na^+ impermeable. Consistently, the time constants of the fast Na^+ current decay were much smaller than for those of the Na^+ current deactivation (Fig. 3) but comparable with those of recovery from inactivation of hERG channels (Zhang et al., 2003a). Since hERG inactivation is voltage dependent, changing the voltage step from 70 mV to less depolarizing voltages would cause recovery of the P-type inactivated channels to the open state. In brief, at steady state during the last pulse in Fig. 4C, the current represents the fraction of channels in the P-type inactivated state. At the beginning of that pulse, there is a relaxation to a lower current level, the reduction of which represents the fraction of channels exiting the inactivated state and moving into the open state. This decrease in current indicates that the Na^+ current does not permeate through the open state.

2.3. Recovery from inactivation

We have shown that Na^+ current displayed a slow inactivation with time constants ranging from 2.7 to 1.6 s at voltages between -20 and 70 mV (Fig. 4A & B). To evaluate the recovery from inactivation, a 6-s depolarizing pulse to 70 mV (P1) was used to induce a "steady-state" inactivation at which no current decay processed. The cells were then repolarized to -80 mV for various periods of time (P2) to recover the inactivated channels to the open state, and then the cells were depolarized to 70 mV for 800 ms (P3) to activate and inactivate the channels to Na^+ permeable state. In this way, the channel

recovery can be measured (Fig. 5A). The more the channels recovered from the inactivated state, the bigger the Na^+ currents could be recorded during P3 pulses. The peak amplitude of the Na^+ current upon P3 was plotted against the duration of P2, and the data points were fitted to the double exponential function to obtain the time constants of recovery from inactivation (τ_{rec}, Fig. 5B). The τ_{rec} at –80 mV were 0.7 ± 0.1 s and 54 ± 12 s (n = 13). Thus, recovery from inactivation of the Na^+ currents is also nearly 1000-fold slower than that of the K^+ current (Zhang et al., 2003a; Lin et al., 2005). These results again indicate that the slow Na^+ current decay may reflect the channel entering into a previously unrecognized 'C-type' inactivation state from which the recovery is slow.

3. Na^+ permeation through inactivated hERG channels

3.1. P-type inactivation state is the Na^+ permeating state

We have recorded robust Na^+ current with Na^+-rich and K^+-free intracellular solution. Inactivation kinetics are very sensitive to permeating ions (Zhang et al., 2003a; Lin et al., 2005). Notably, a K^+ free, Na^+ rich intracellular condition is very different from physiological conditions. To support our hypothesis that the hERG Na^+ current represents Na^+ permeating through the inactivated channels, it is fundamental to validate that hERG channels still display the characteristic fast, voltage dependent inactivation under this extreme circumstance.

To address the hERG inactivation in the absence of K^+ but with 135 mM Na^+ in the pipette solution, the pulse protocols shown in Fig. 6 A and B were used. A bath solution

containing 5 mM K^+ and 130 mM NMG^+ was used to study the hERG inactivation by monitoring the inward K^+ current. The hERG channels were inactivated by a holding potential of 60 mV. Repolarization to −100 mV (P1) induced channel recovery from the inactivated to the open state (K^+ permeable state) and the maximum inward K^+ current could be recorded. Before deactivation, the cell membrane was depolarized to 20 mV (A) or 60 mV (B) with various durations (P2) to induce channel inactivation (the longer the duration, the more the channels inactivated). Since inactivation state is K^+ impermeable, the more the channels are inactivated, the smaller the inward K^+ currents could be recorded upon depolarization steps. The cell membrane voltage was then repolarized back to −100 mV (P3). The instantaneous inward K^+ current immediately after the membrane capacitive current upon P3 represents the fraction of not-yet-inactivated open channels, which decreases as the preceding depolarization to 20 or 60 mV (P2) was prolonged (Fig. 6 A & B), reflecting the time dependent inactivation occurring at depolarizing voltages (P2). Fitting the time course of the instantaneous current decrease gave a time constant for channel inactivation at 20 mV (Fig. 6A) or 60 mV (Fig. 6B). The time constants of inactivation at different depolarizing voltages were assessed and summarized in Fig. 6D (●, n = 5). The voltage dependent inactivation of hERG channels with 135 mM K^+ in the pipette solution (bath solution containing 5 mM K^+) was also evaluated using the standard triple pulse protocol (Fig. 6C) and also plotted in Fig. 6D (○, n = 4). Although the onset of hERG channel inactivation with 135 mM Na^+ in the pipette solution was faster than that with 135 mM K^+ in the pipette solution, hERG channels with 135 mM Na^+_i displayed unique fast, voltage dependent inactivation similar to those with 135 mM K^+_i.

To directly address the hypothesis that the Na^+ permeation state is the initial P-type inactivated state, we performed experiments with a pipette solution containing 135 mM Na^+ (135 mM Na^+_i) and a bath solution containing 135 mM NMG^+ plus 1 mM K^+ (1 mM K^+_o). Under these recording conditions, depolarizing step to 80 mV evoked a small sustained outward Na^+ current (Fig. 7A). The small amplitude of the outward Na^+ current resulted from the blocking effects of 1 mM K^+ in the external solution (see Fig. 2). Repolarizing steps elicited inward K^+ tail currents. Since K^+ only permeates through open channels, the shape of the inward tail current upon repolarization would provide us with critical information. If the Na^+ permeating state is the open state during the depolarizing step, the repolarization would evoke an instantaneous inward K^+ current. On the other hand, if the Na^+ permeating state is the fast P-type inactivated state, the tail current would display a rising phase, which reflects the fast P-type inactivated channels recovering to open state and then deactivating (recovery is faster than deactivation). The data shown in Fig. 7A-C clearly indicate that the latter is the case. During depolarization to 80 mV, a sustained Na^+ current was recorded. Repolarizations to various voltages induced the inward tail currents which displayed a rising phase prior to the current deactivation. The initial portion of the tail current is expanded in Fig. 7B to show the rising phase of the tail currents. To obtain the recovery time constants, the rising phase of the tail current was fitted to a single exponential function. The time constants, which were plotted against the voltages in Fig. 7C, displayed characteristic voltage dependence (n = 6). The voltage dependent rising phase of the tail currents is usually referred to as the "hook" which is unique to hERG channels, and reflects the channel recovery from the inactivated state to the open state. The recovery time constants of the hERG channel were also evaluated

with a pipette solution containing 135 mM K^+ and a bath solution containing 135 mM NMG^+ plus 1 mM K^+ (135 mM K^+_i\1 mM K^+_o, Fig. 7D-F, n = 7). Although recovery from inactivation of hERG channels is faster with 135 mM Na^+_i than that with 135 mM K^+_i, it is clear that the hERG channel displayed its unique fast voltage dependent recovery from inactivation when the 135 mM Na^+ containing pipette solution was used.

In summary, data in Fig. 6 & 7 indicate that the hERG channel displayed its unique fast voltage dependent inactivation and recovery from inactivation when a K^+ free, 135 mM Na^+ pipette solution was used. The onset of and recovery from inactivation described here is equivalent to the gating transitions between open and P-type inactivation state. Thus, the P-type inactivation state likely represents the Na^+ permeating state.

3.2. Properties of Na^+ current in hERG inactivation-affected mutant channels

If the Na^+ permeating state is the inactivated state, then accelerating inactivation would not significantly affect the Na^+ current because the inactivation is faster than activation in WT channels, and thus the channel activation is the rate-limiting step for the appearance of the Na^+ current upon depolarizations. On the other hand, disruption of the fast (P-type) inactivation would eliminate the Na^+ permeation. These rationales were experimentally addressed below.

The T623A and S641A mutations have been reported to accelerate hERG channel inactivation (Mitcheson et al., 2000; Bian et al., 2004). We recently found that the F627Y mutation accelerates hERG inactivation (Guo et al., 2006). In T623A, F627 Y or S641A

mutant channels when a pipette solution containing 135 mM K^+ was used, no K^+ current could be recorded with a bath solution containing 5 mM K^+_o, but a robust WT channel current was recorded (Fig. 8, left panel). Since K^+ ions can not permeate through inactivated channels, the accelerated inactivation in the mutant channels limited the outward flux of K^+ ions. Thus, K^+ current could not be recorded in T623A, F627 Y or S641A mutant channels. As has been reported (Sanguinetti et al., 1995; Yang et al., 1997a), we found that removal of external K^+ led to a drastic reduction of the WT hERG current (Fig. 8, right panel). Please note the different scale bars for the top current traces. Also see the bottom panels for the summarized data). Consistent with the 'C-type' inactivation of the hERG Na^+ current (Fig. 4), two features of the WT K^+ current traces in the absence of K^+ suggest the entry into 'C-type' inactivation of the channel when the "physiological" intracellular solution (135 mM K^+) was used. First, decays of the hERG current appear upon 4 s depolarizations (Fig. 8, right panel, top traces). Second, the tail current in the absence of K^+_o is much smaller than that in the presence of K^+_o. Because recovery from P-type inactivation is fast enough to generate a unique hERG tail current, the small tail in the absence of K^+_o indicates that majority of hERG channels had entered into a state from which recovery is not fast enough to generate tail current.

For the T623A, F627Y and S641A mutant hERG channels, as we confirmed below, the virtual absence of any detectable K^+ current was due to the very fast entry into the P-type inactivated state. The absence of tail currents also suggests that either the deactivation is accelerated, which means that channels close so fast that there is no time for K^+ ions to flow out to generate tail currents, or the recovery from inactivation is decelerated. To

directly confirm that the absence of K^+ current in these mutant channels is a consequence of accelerated P-type inactivation, we investigated the gating kinetics of these channels. hERG K^+ currents were recorded under symmetrical 135 mM K^+ conditions under which inward tail currents were present upon repolarization to -80 mV after channel activation (Fig. 9, left panel). The decay of the tail currents reflecting channels closed from the open state upon repolarization (deactivation) was fitted to a single exponential function to estimate the deactivation time constant (τ_{deact}). It was found that τ_{deact} at -80 mV was 993.4 ± 264.9 ms for WT channels (n = 5), 62.3 ± 4.6 ms for T623A (n = 7), 151.4 ± 20.2 ms for F627Y (n = 10), and 94.7 ± 17.0 ms for S641A (n = 8). Thus, the deactivation was significantly accelerated in all three mutant channels ($p<0.01$). We also analyzed the time course of recovery from inactivation in WT and mutant channels. The rising phase of the tail current at −80 mV reflecting channels opened from the inactivated state upon repolarization (recovery from inactivation) was fitted to a single exponential function to obtain the time constant of recovery from inactivation (τ_{rec}). The τ_{rec} at −80 mV was 7.9 ± 0.8 ms (n = 5), 3.1 ± 0.3 ms (n = 8), 3.0 ± 0.3 ms (n = 12), and 2.9 ± 0.4 ms (n = 8) for WT, T623A, F627Y and S641A channels, respectively. Thus, the recovery from inactivation was accelerated in the three mutant channels ($p<0.01$). To construct the activation curve, the tail current peak amplitudes were plotted against the activation voltages and the data points were fitted to the Boltzmann equation. The voltage of half-activation of the channel ($V_{1/2}$) and the slope factor (k) were −11.6 ± 1.2 mV and 6.8 ± 0.4 mV for WT channels (n = 5), 2.9 ± 4.1 mV and 7.6 ± 0.6 mV for T623A (n = 7), −18.7 ± 3.9 mV and 8.7 ± 0.4 mV for F627Y (n = 6), and −4.2 ± 2.7 mV and 7.1 ± 0.4 mV for S641A (n = 6). Compared to WT channels, the $V_{1/2}$ of F627Y was not

significantly changed ($p>0.05$), and those of the T623A and S641A were slightly shifted to the positive direction (Fig. 9, $p<0.05$, bottom in the left panel). To evaluate inactivation time course of these mutant channels, a triple-pulse protocol was used. The hERG current decay during the test voltages was fitted to a single exponential function, and the time constant of inactivation (τ_{inact}) was plotted against the test voltages (Fig. 9 right panel). Compared to WT channels, inactivation was dramatically accelerated in all three mutants. For example, the τ_{inact} at 50 mV was increased by 12.6 (n = 7), 6.1 (n = 6), and 6.1 folds (n = 7) by the T623A, F627Y and S641A mutation, respectively. These results indicate that the absence of hERG T623A, F627Y and S641A K^+ currents at 0 or 5 mM K^+_o was due to an accelerated inactivation as well as an accelerated deactivation.

In contrast to K^+ currents, robust outward Na^+ currents were recorded in T623A, F627Y and S641A channels (Fig. 10). The relative peak current-voltage relationships are shown in Fig. 10B. The activation time courses of the Na^+ current in these three mutant channels were analyzed by single exponential fitting of the final rising portion of the current activation, a similar approach which was used in WT channels (Fig. 3). Whereas the activation time courses were similar between WT and S641A mutant Na^+ currents, activation time courses of T623A and F627Y were slower than that of WT channels (Fig. 10C). Because the mutant T623A, F627Y, S641A channels displayed a significantly accelerated inactivation (Fig. 9), the presence of Na^+ current in these mutant channels strongly supports the notion that Na^+ permeating state represents the inactivated state.

To further address the inactivation state is the Na^+ permeation state, we made the S631A

mutation. This mutation is known to disrupt fast voltage-dependent hERG inactivation but retains high K^+ selectivity (Schönherr et al., 1996; Fan et al., 1999). We found that no detectable Na^+ current could be recorded in S631A inactivation-deficient channels (Fig. 11A). The function of S631A channels was confirmed by adding 1 mM K^+ to the bath solution, which caused an inward tail current upon repolarization to –80 mV without the rising phase that is present in WT channels (Fig. 11B). This immediate inward tail current with a sharp decrease upon repolarization reflected the channels directly closed from the open state. This result indicated that the S631A channels were in the open state during the depolarizing pulse. Since no Na^+ current could be recorded in S631A channels upon depolarization, Na^+ ions could not permeate through the open hERG channels.

4. Inhibition of the hERG Na^+ current by external Na^+ ions

During the course of experiments, we were never able to record inward Na^+ current in WT hERG channels. We found that external Na^+ in fact potently blocks the hERG Na^+ current. As shown in Fig. 12A, a family of Na^+ currents was recorded with a bath solution containing 135 mM NMG^+ (pipette solution contained 135 mM Na^+). When 10 mM Na^+ was added to the bath solution (NMG^+ was proportionally reduced), the Na^+ current was considerably reduced (Fig. 12B). The reduction of the outward Na^+ current was not simply due to the decreased driving force because the maximal current was reduced and the inward Na^+ current never appeared. The concentration-dependent effects of external Na^+ on hERG Na^+ current were examined, and the half maximal concentration (IC_{50}) for external Na^+ to block the outward Na^+ current was 3.5 $\pm$ 0.4 mM (Fig. 12C, n = 8). The Hill coefficient was 0.7, suggesting that one Na^+ ion binding to the channel can

cause the block.

External Na^+ has been reported to block hERG K^+ current and the S624 residue was proposed to be involved in the block (Mullins et al., 2002). We found that the S624A mutation removed the inhibitory effects of Na^+_o on the Na^+ current of hERG channels. In addition, we found that the F627Y and S641A mutations also abolished the blocking effects of external Na^+ on the hERG Na^+ current. However, Na^+_o still blocked the T623A Na^+ current with potency similar to that of WT channels (data not shown). As can be seen in Fig. 13, in the symmetric Na^+ solutions (135 mM Na^+), no current could be detected in WT channels. In contrast, Na^+ currents were present in both inward and outward directions in mutant channels S624A, F627Y and S641A (n = 4-9 cells for each mutation). Thus, although changes of the reversal potential at varying external Na^+ concentrations could not be determined in WT hERG channels due to the external Na^+ blocking effect, they were examined in S624A, F627Y and S641A mutants (Fig. 14). The slope factor of the linear fit to the data was 39.8 ± 5.3 (n = 6) for S624A, 55.7 ± 3.7 (n = 4) for F627Y and 46.9 ± 4.5 (n = 5) for S641A. Compared to the value (58.3) predicted by Nernst equation for Na^+ permeation, the slope factor for F627Y was not different and those for S624A and S641A were smaller ($p<0.05$). Despite the difference, the fact that changing external Na^+ concentrations alters the reversal potentials of the Na^+ currents in these three mutant channels indicate that it is indeed Na^+ that permeates the mutant hERG channels.

To directly explore the state that Na^+_o permeates in the S624A, F627Y and S641A mutant

channels, we focused on the F627Y mutant channel to investigate the inward Na^+ tail current and compared it with the K^+ tail current (Fig. 15). Following channel activation, the K^+ tail current displayed a rising phase reflecting recovery of inactivated channels to the open state prior to deactivation (Fig. 15B). In contrast, the Na^+ tail current did not display such a rising phase and reached the peak amplitude immediately upon repolarization and then deactivated (Fig. 15A). These results indicate that Na^+ ions permeate through the inactivated state of F627Y channels. To examine the voltage dependence of the F627Y activation, the peak amplitudes of the tail currents were plotted against the depolarizing voltages, and g-V relationships were obtained (Fig. 15C). It was found that the g-V relationship of the Na^+ current was bell-shaped. The Na^+ tail current increased to reach the maximal value and then decreased following stronger depolarizations, indicating the entry into the stabilized 'C-type' inactivation, from which recovery is slow. For K^+ current, the tail current reached the maximal value at 10 mV and remained constant at more positive voltages (Fig. 15C). The g-V relations of the Na^+ and K^+ currents were fitted to the Boltzmann function. The $V_{1/2}$ and k of the K^+ current were -18.7 ± 0.9 mV and 8.8 ± 0.4 mV, respectively ($n = 6$), and the $V_{1/2}$ and k of the Na^+ current were -30.7 ± 1.6 mV and 6.7 ± 0.7 mV, respectively ($n = 6$). Thus, the $V_{1/2}$ of the Na^+ current is more negative than that of the K^+ current ($p<0.01$).

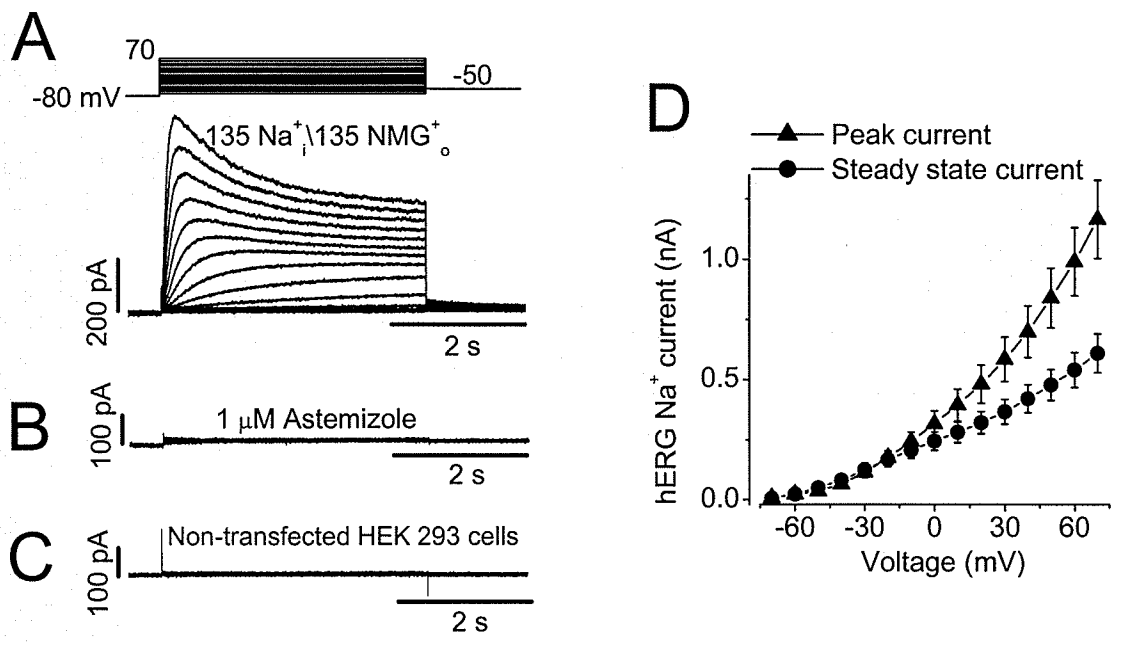

Figure 1. Na^+ permeation through hERG potassium channels. **A**: Na^+ currents were elicited by depolarizing voltage steps from hERG channels stably expressed in HEK 293 cells. The pipette solution contained 135 mM Na^+ and the bath solution contained 135 mM NMG^+ as major cations. **B**: Na^+ currents recorded from the hERG-HEK 293 cells were completely blocked by 1 μM astemizole, a specific hERG blocker. **C**: No Na^+ current could be detected in the non-transfected HEK 293 cells. **D**: Current-voltage (I-V) relationships for the peak (▲) and steady state (●) hERG Na^+ currents recorded during the 4-s depolarization pulses (n = 13, data points and error bars signify mean ± S. E. M.). **These results indicated that the Na^+ currents in A reflected Na^+ ions permeation through hERG channels.**

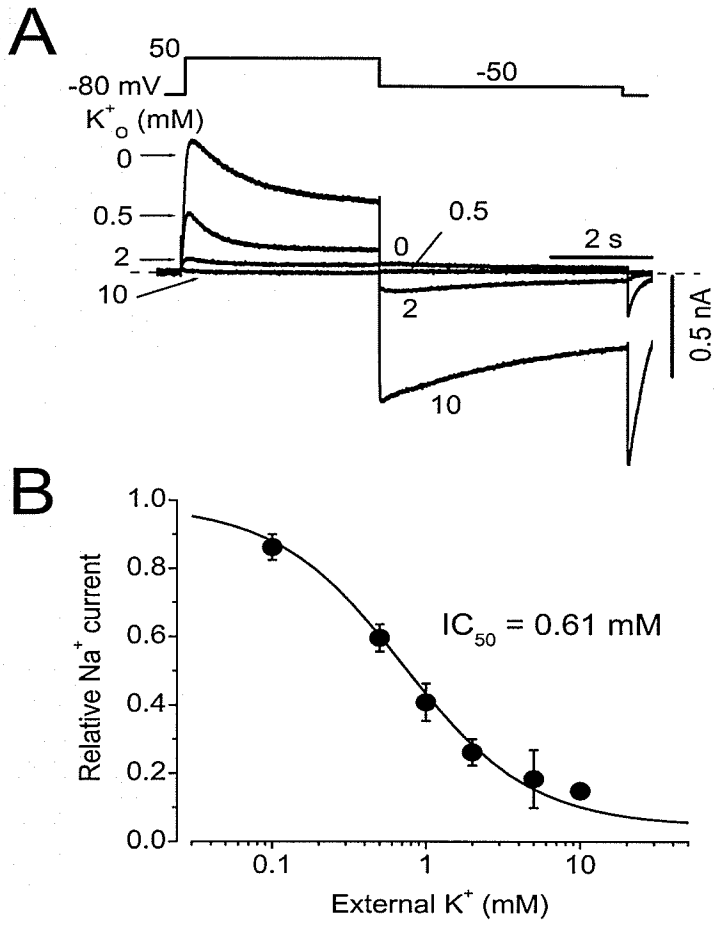

Figure 2. Inhibition of hERG Na^+ currents by extracellular K^+ (K^+_o). **A**: Superimposed current traces with constant 135 mM Na^+_i and varying K^+_o. **B**: Concentration dependent inhibition of outward Na^+ currents by K^+_o (n = 7). **The outward currents in A were Na^+ currents while the inward currents were generated by influx of external K^+ ions. The appearance of the inward K^+ tail currents suggests that hERG channels are intact when Na^+ permeates.**

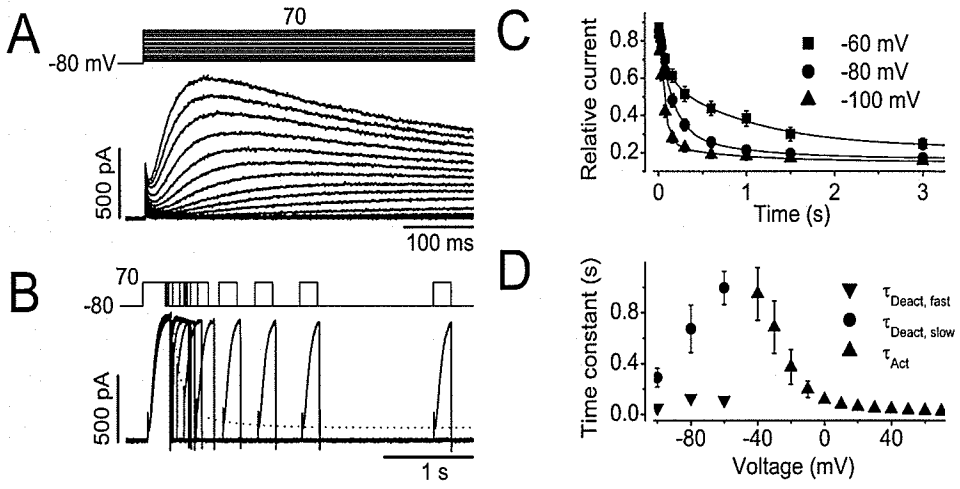

Figure 3. Time courses of hERG Na^+ current activation and deactivation. **A**: The initial phase of the Na^+ currents during the depolarizing pulses ranging from -70 to 70 mV in 10 mV increments. The activation time constants were estimated by fitting the rising phase of each current trace to a single exponential function with the initial sigmoidal component ignored (n = 13). **B**: A three-pulse protocol was used to study the hERG Na^+ current deactivation. After a peak current was reached by the initial depolarizing pulse to 70 mV (P1), the cell was clamped to -80 mV (P2) for different periods of time before it was depolarized to 70 mV (P3) to monitor the channel deactivation. The dotted line indicates the double exponential fit to the instantaneous current amplitudes upon P3. **C**: The amplitude of the initial current during P3 was plotted against the time periods of P2 at -60, -80 and -100 mV, fitted to double exponential functions to obtain time constants of deactivation at -60 (■),-80 (●) and -100 mV (▲) (n = 7). **D**: Voltage dependence of the time constants of activation (▲), and fast (▼) and slow (●) components of deactivation. **Two of the basic electrophysiological properties of hERG Na^+ current were shown, activation and deactivation.**

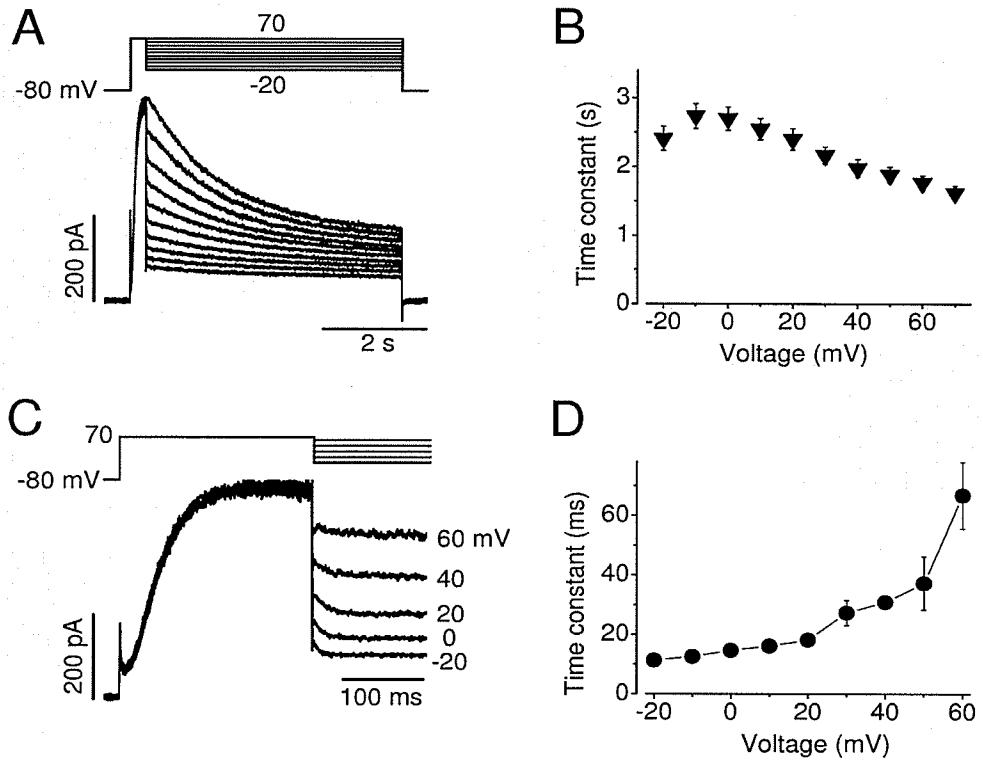

Figure 4. Voltage dependent fast and slow decay of the hERG Na^+ current. **A**: Cells were held at -80 mV and depolarized to 70 mV for 250 ms to induce the maximal hERG Na^+ currents. Test pulses were followed at potentials ranging from -20 to 70 mV in 10 mV increments. Current decays during 5-s test pulses were fitted to a single exponential function to obtain the time constants. **B**: Voltage dependence of the averaged slow decay time constants from 9 cells. **C**: hERG Na^+ current during the voltage changes from 70 mV to various test potentials. hERG Na^+ current was evoked by a depolarizing step to 70 mV for 250 ms, immediately followed by test potentials between -20 and 60 mV. The rapid decay of the Na^+ current upon various test potentials was fitted to a single exponential function to obtain time constants. **D**: The voltage dependence of the time constants of the rapid Na^+ current decay (n = 6 cells for each voltage). hERG currents were recorded with a pipette solution containing 135 mM Na^+ and a bath solution

containing 135 mM NMG^+. **The slow current decay in A represents the slow inactivation of hERG Na^+ current while the fast current decay in C represents the recovery of P-type inactivated channels (Na^+ permeable) to the "open" state which is Na^+ impermeable.**

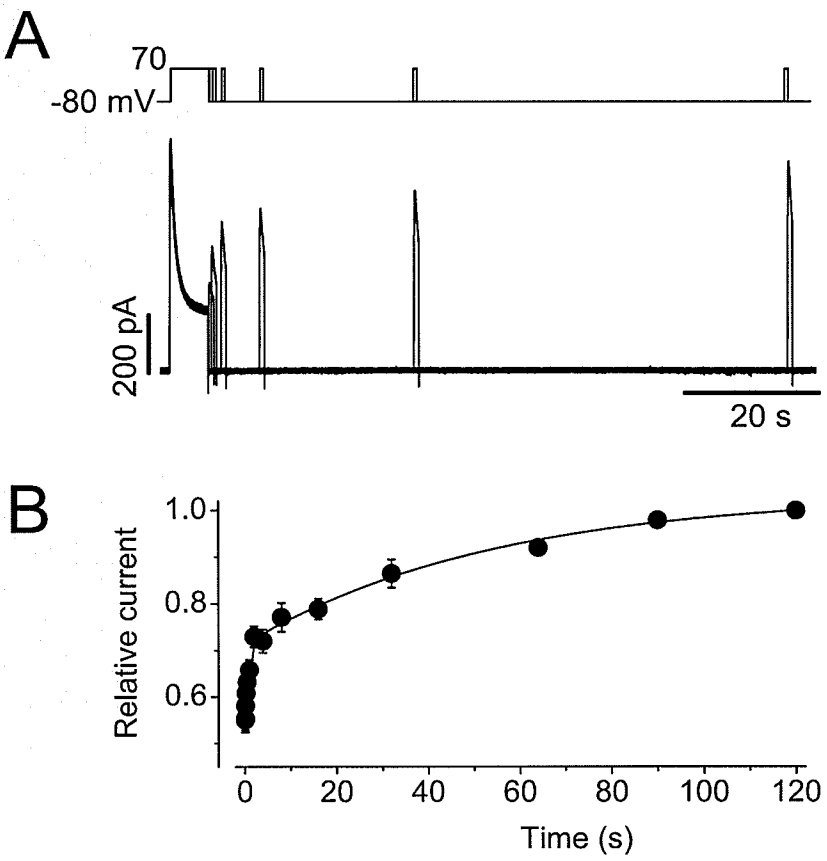

Figure 5. Time course of recovery from inactivation of the hERG Na^+ current. A: Voltage protocol and the Na^+ currents for studying recovery from inactivation. From a holding potential of -80 mV, the cell was depolarized to 70 mV for 6 s until steady state inactivation was reached. The cell was then clamped to -80 mV for different periods of time before it was depolarized to 70 mV for 800 ms to observe channel recovery. The inter-pulse interval was 120 s. **B**: Time dependent recovery of the Na^+ current. The superimposed line represents the best fit of the averaged data from 13 cells to double exponential functions. **This result indicated that recovery from inactivation of the Na^+ currents is very slow.**

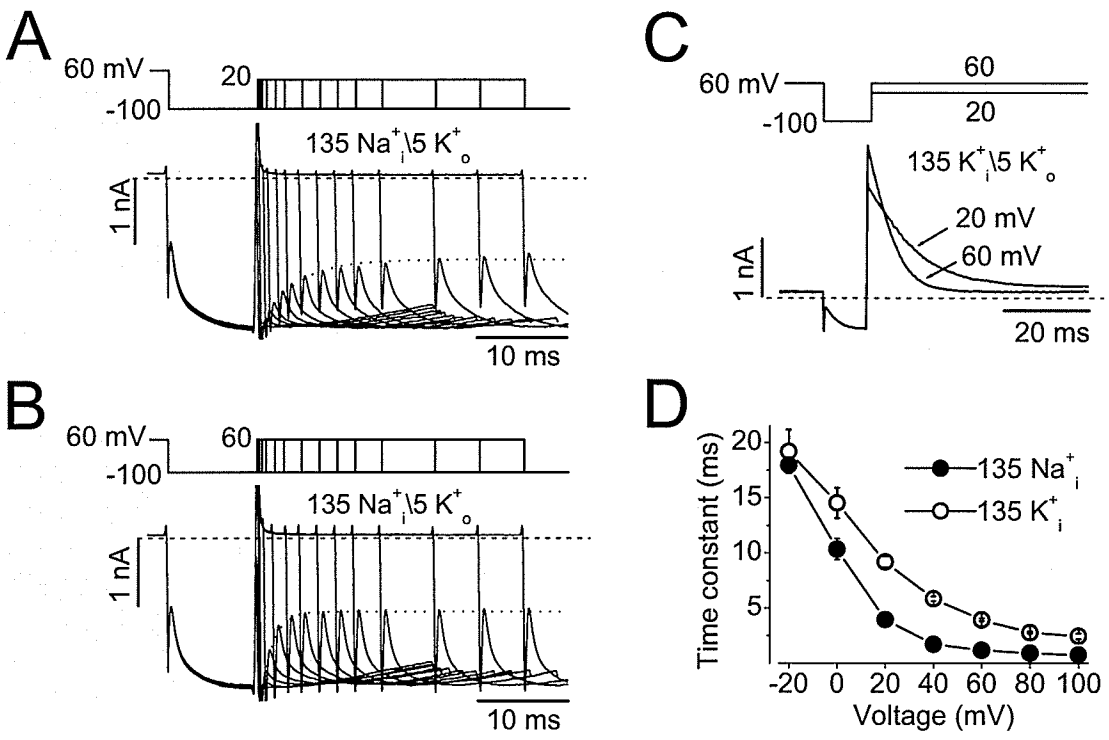

Figure 6. Voltage dependent inactivation of hERG channels in the presence of 135 Na^+_i (A, B & D) or 135 mM K^+_i (C & D). A & B: hERG currents evoked by the voltage protocol shown above the traces to monitor the time dependent channel inactivation at 20 (A) or 60 mV (B). hERG channels were inactivated at the holding potential of 60 mV. Repolarization to -100 mV (P1) caused channel recovery from inactivation. The membrane was depolarized to 20 or 60 mV with increasing durations (P2) to induce the voltage dependent inactivation which was judged by the instantaneous currents upon repolarization to -100 mV (P3) after P2. The instantaneous currents immediately after the cell capacitive current upon P3 were fitted to the single exponential function (dotted lines) to obtain the inactivation time constants. **C:** Inactivation time courses of the hERG outward K^+ current at 20 or 60 mV. hERG channels were inactivated at the holding potential of 60 mV. Repolarization to -100 mV induced channel recovery from

inactivation. The membrane was then depolarized to 20 or 60 mV to induce current inactivation which was fitted to a single exponential function. **D:** Inactivation time constant-voltage relationships of hERG channels under 135 Na^+_i / 5 mM K^+_o (●, n = 5) or 135 mM K^+_i / 5 mM K^+_o (○, n = 4). **hERG inactivation in the absence of K^+ but with 135 mM Na^+ in the intracellular solution is similar to the characteristic fast, voltage-dependent inactivation under the physiological solution.**

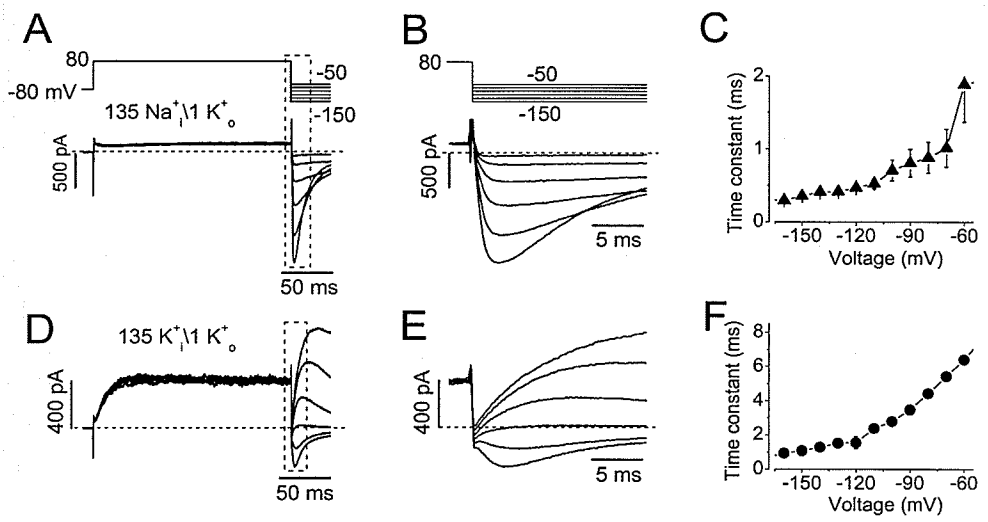

Figure 7. Recovery from inactivation of hERG channels under conditions of 135 mM Na^+_i \ 1 mM K^+_o (A-C) or 135 mM K^+_i \ 1 mM K^+_o (D-F). hERG currents were recorded with a bath solution containing 1 mM K^+ plus 135 mM NMG^+ and a pipette solution containing either 135 mM Na^+ (A-C) or 135 mM K^+ (D-F). **A**: hERG outward Na^+ currents and the inward K^+ currents elicited by the voltage protocol above the current traces. **B**: The expansion of initial phase of the tail currents. The rising phase of the tail current upon repolarization reflects the fast recovery of the inactivated channels to the open state before deactivation. The rising phase of the tail current was fitted to a single exponential function to obtain the time constant of recovery from inactivation (τ_{rec}) at each voltage. **C**: The τ_{rec}-voltage relationships under 135 mM Na^+_i \ 1 mM K^+_o (n = 6). **D**: hERG outward and inward K^+ currents elicited by the same voltage protocol shown at the top of panel A. **E**: The expansion of initial phase of the tail currents. The rising phase of the tail current was fitted to a single exponential function to obtain the time constant of recovery from inactivation (τ_{rec}) at each voltage. **F**: The τ_{rec}-voltage relationships under 135 mM K^+_i \ 1 mM K^+_o (n = 7). **The tail current in B displayed a rising phase, which reflected Na^+ permeating through the fast P-type inactivated state.**

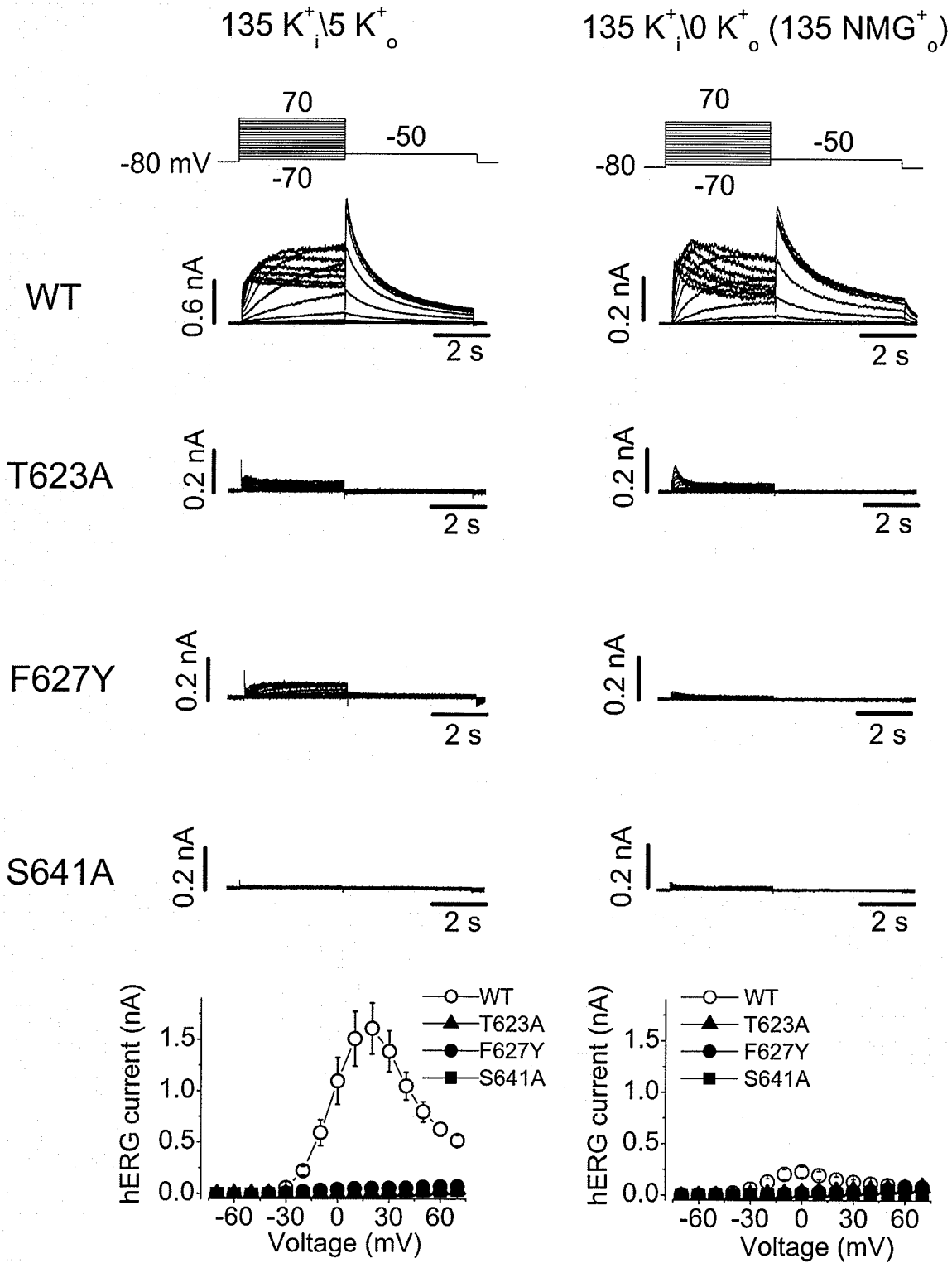

Figure 8. Families of WT, T623A, F627Y and S641A hERG K^+ currents recorded in the presence of 5 mM K^+_o (left panel) or in the absence of K^+_o (NMG^+ as substitute,

right panel). The pipette solution contained 135 mM K^+. In both panels, the voltage protocols are shown at the top and the current-voltage relationships are shown at the bottom. Changing external K^+ from 5 mM to 0 significantly reduced the WT hERG current (note the different bar scales in WT current traces in 0 and 5 mM K^+). **In both 5 mM and 0 K^+_o conditions, no significant current could be recorded in the T623A, F627Y and S641A mutant hERG channels (n = 4-7 cells), which was due to the acceleration of hERG inactivation by these three mutant channels.**

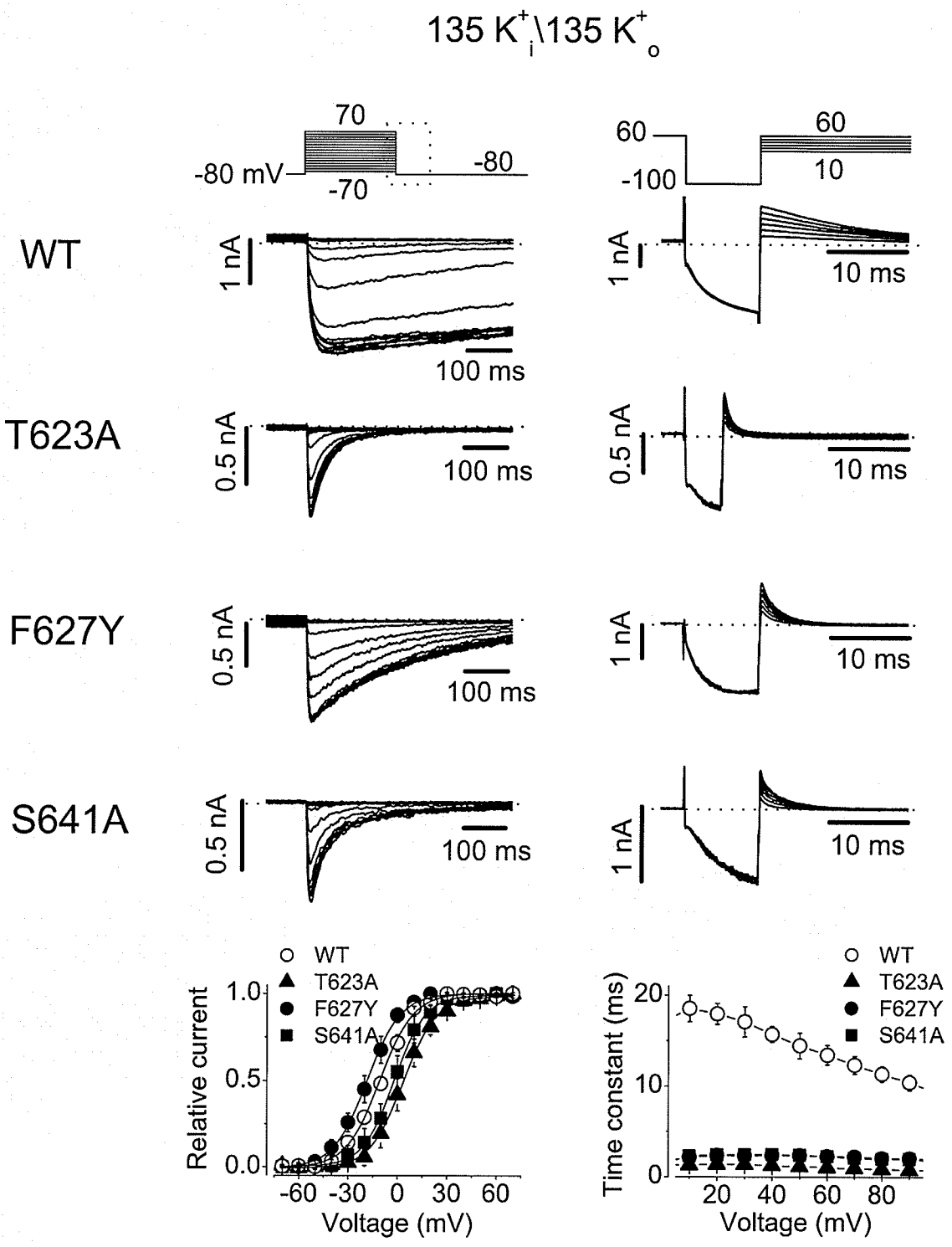

Figure 9. Gating properties of WT, T623A, F627Y and S641A hERG channels under symmetrical K^+ conditions. Both pipette and bath solutions contained 135 mM

K^+. The voltage protocols are shown at the top of each panel. **Left panel:** Activation properties of various hERG channels. Note that only a portion of the tail currents corresponding to the boxed area in the voltage protocol is shown. Peak tail currents were plotted against the test voltages and fitted to a Boltzmann function to obtain the activation curves. The rising and the decay phases of the tail currents were fitted to the single exponential function, respectively, to obtain the time constant of recovery from inactivation and to estimate the deactivation time course. Compared to WT channels, the deactivation of all three mutant channels was significantly faster. **Right panel:** Inactivation properties of various hERG channels. The current decay upon each test voltage was fitted to a single exponential function to obtain the inactivation time constants (τ_{inact}) which are plotted against the depolarizing voltages at the bottom of the panel. **The T623A, F627Y and S641A mutations drastically accelerated hERG inactivation at all tested voltages.**

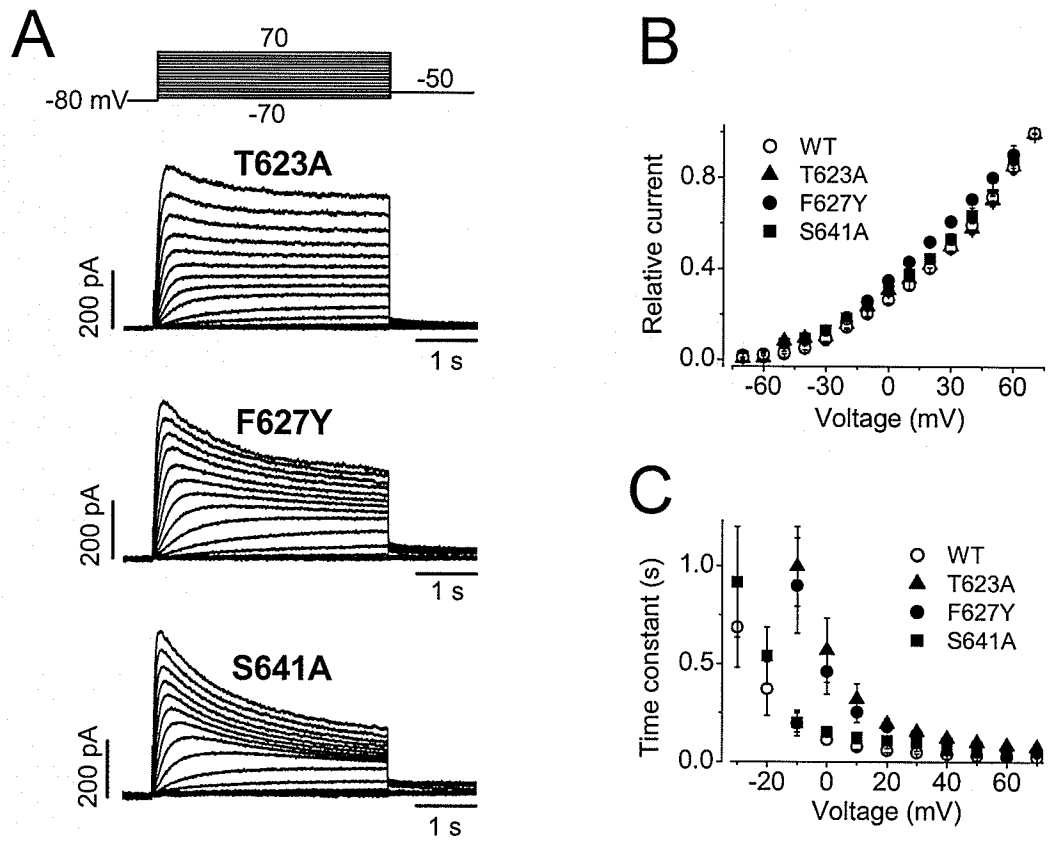

Figure 10. Na^+ currents recorded from the T623A, F627Y and S641A mutant hERG channels. **A**: Families of Na^+ currents from T623A, F627Y and S641A. **B**: The relative current-voltage relationships of Na^+ currents recorded from WT, T623A, F627Y and S641A channels (n = 5-9 cells). **C**: The activation time constant-voltage relationships of the T623A, F627Y and S641A Na^+ currents (n = 5-9 cells), data for WT channels were also shown for comparison (n=13). **In contrast to K^+ currents, robust outward Na^+ currents were recorded in T623A, F627Y and S641A channels, which demonstrated that Na^+ permeates through the inactivation state.**

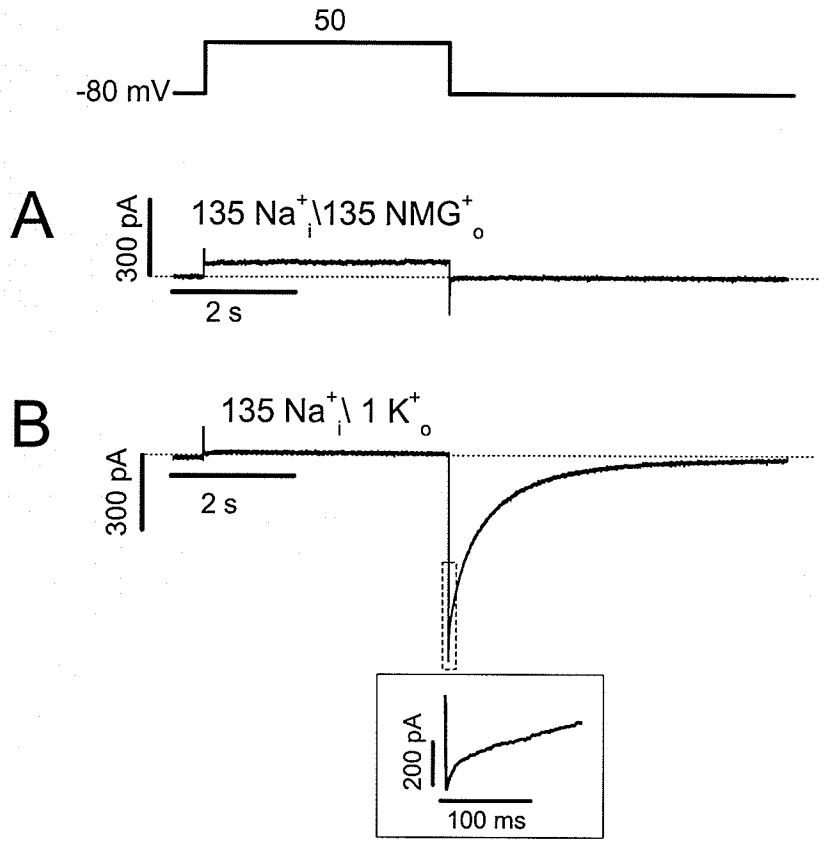

Figure 11. Absence of Na^+ current in the inactivation-deficient mutant hERG channel, S631A. A: Current recorded with the pipette solution containing 135 mM Na^+ and the bath solution containing 135 mM NMG^+. **B**: Current recorded with the similar condition but with 1 mM K^+ added to the bath solution (n = 4). The portion of the tail current in the dotted box is expanded in the inset to show the absence of the rising phase of the S631A K^+ tail current. **No Na^+ current could be recorded in S631A inactivation-deficient mutant channels, which further confirmed that Na^+ permeation state is the inactivation state.**

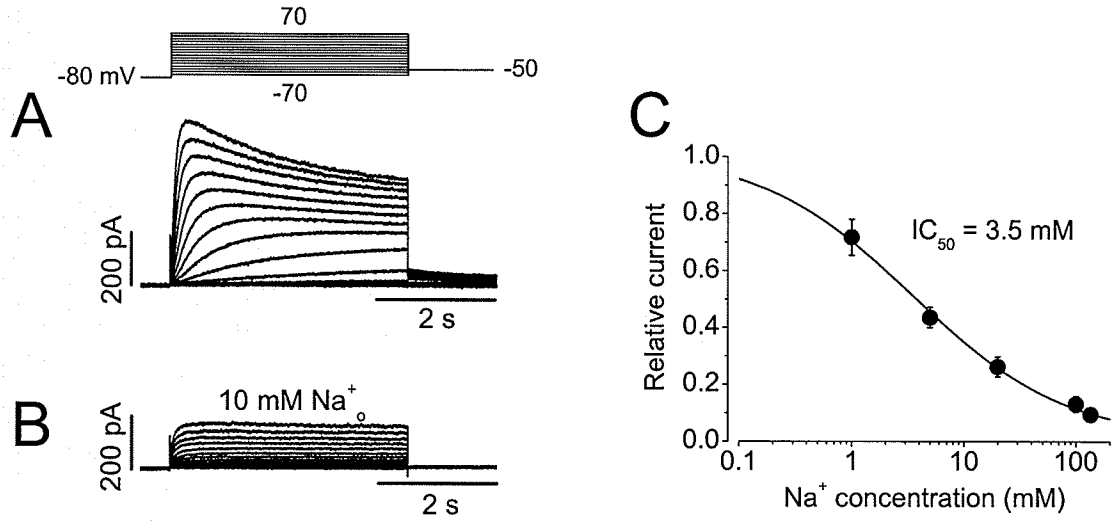

Figure 12. Inhibition of hERG Na^+ currents by external Na^+ ions (Na^+_o). A & B: hERG Na^+ currents in the absence (**A**) and presence of 10 mM Na^+_o (**B**). The pipette solution contained 135 mM Na^+. **C**: The concentration-dependent block of hERG Na^+ current by Na^+_o. The outward Na^+ currents at 50 mV at each Na^+_o relative to the control value were plotted against the Na^+_o concentration, and the data were fitted to the Hill equation (n = 8). **These data revealed that external Na^+ blocked the hERG Na^+ current.**

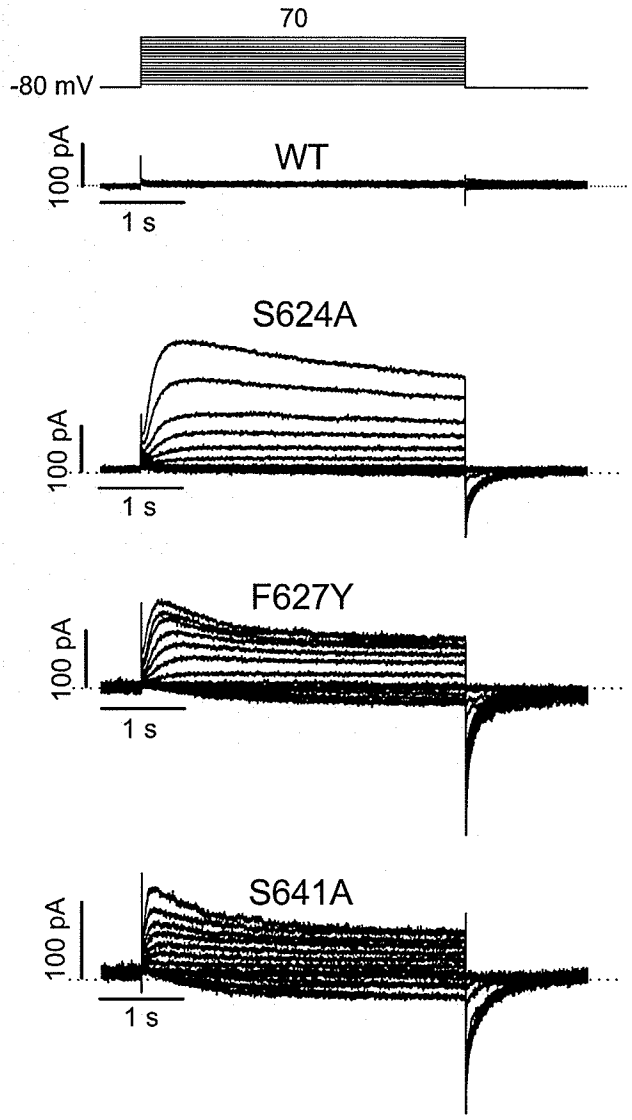

Figure 13. The S624A, F627Y and S641A mutations eliminated Na^+_o induced blockade of the hERG Na^+ current. Families of Na^+ currents from the WT, S624A, F627Y and S641A channels in the symmetric Na^+ solutions (135 mM Na^+ in the pipette and bath solutions). The channels were activated by voltage steps from -70 to 70 mV in 10 mV increments from the holding potential of -80 mV. The cell was then clamped to -80 mV to elicit the tail currents. **In contrast to WT channels, 135 mM Na^+_o did not block the S624A, F627Y and S641A Na^+ currents which were present in both inward and outward directions.**

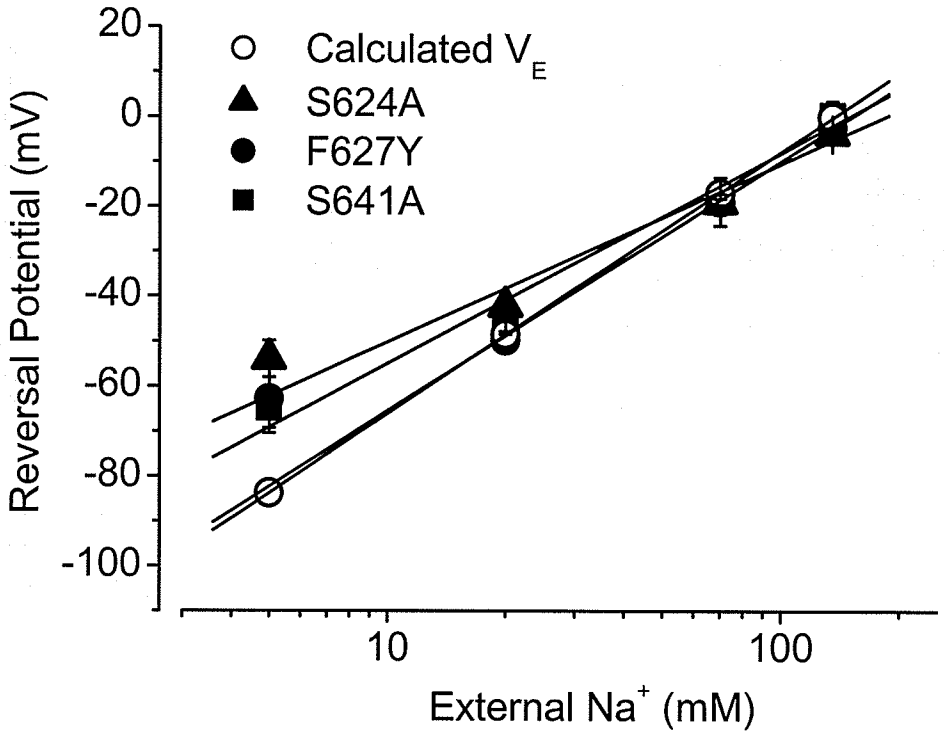

Figure 14. The reversal potentials of the S624A, F627Y and S641A hERG channels under 135 mM intracellular Na^+ and varying external Na^+ concentrations. For each mutation, 4-6 cells were tested. The predicted reversal potential values (calculated V_E) were also shown. **The overlap of sodium reversal potentials of the S624A, F627Y and S641A hERG channels with the calculated sodium reversal potential indicated that it is indeed Na^+ that permeates through the mutant hERG channels.**

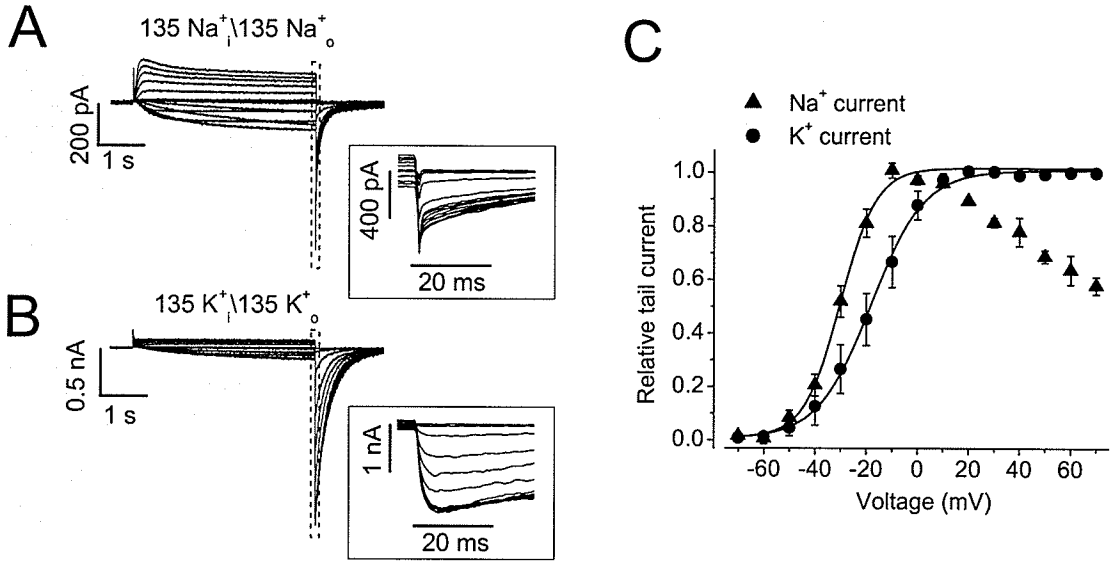

Figure 15. Comparison of the F627Y Na^+ and K^+ currents. Families of the Na^+ currents (Na^+_i\$Na^+_o$ 135 mM, **A**) and K^+ currents (K^+_i\$K^+_o$ 135 mM, **B**) from F627Y mutant channels. The channels were activated by voltage steps from -70 to 70 mV in 10 mV increments from the holding potential of -80 mV. The cell was then clamped to -80 mV to elicit the tail currents. The portions of the tail currents in the dotted box were expanded in the inset of **A** and **B**, respectively. The tail current-activation voltage relationships (g-V) were shown in **C**. The data points of K^+ currents at all tested voltages as well as those of Na^+ currents between -70 and -10 mV were fitted to the Boltzmann equation. **By comparing and analyzing of the F627Y Na^+ and K^+ currents, we conclude that Na^+ ions permeate through the inactivated state of F627Y channels.**

VI. DISCUSSION

In the present study, we have demonstrated the existence of a robust Na^+ current in WT hERG channels. It is well known that hERG inactivation is voltage dependent; stronger depolarizations inactivate more channels. However, we found that stronger depolarization induced a larger outward Na^+ current in WT hERG channels. In the mutant T623A, F627Y and S641A channels, the inactivation was accelerated to such an extent that outward K^+ current was not detectable under 0 or 5 mM K^+_o condition (Fig. 8). However, robust Na^+ currents were recorded in these mutant channels (Fig. 10). These results indicate that Na^+ permeates through an inactivated state of the hERG channel. Our data further showed that the hERG Na^+ current displayed an inactivation which is different from the well documented fast voltage-dependent hERG inactivation. This inactivation was slow (τ in a range of seconds) and displayed very weak voltage dependence. Recovery from this slow inactivation was also much slower than that of hERG K^+ current.

We propose that the hERG inactivation involves at least two steps, the P-type inactivation (I^P) and the 'C-type' inactivation (I^C, Fig. 16). The well documented fast voltage-dependent inactivation of the hERG K^+ current may represent the I^P, but I^C has not been described possibly because it is prevented by external K^+ ions. As previously reported, K^+_o also slows the entry into I^P (Zhang et al., 2003a). We propose that I^P involves a constriction of the channel pore in a limited region, and that this local conformational change excludes K^+ permeation. However, such partially constricted pore mouth still

allows passage of smaller Na^+ ions. I^P state is less stable and does not involve charge immobilization. The onset and recovery from I^P are fast. In our Na^+ current recording, I^P is manifested by the appearance of the Na^+ current. The slow inactivation of the Na^+ current represents transition from I^P to I^C, a stabilized state causing charge immobilization and involving a more substantial conformational change of the channel that locks the voltage sensor in an outward position. I^C is Na^+ impermeable. The onset and recovery from I^C are slow.

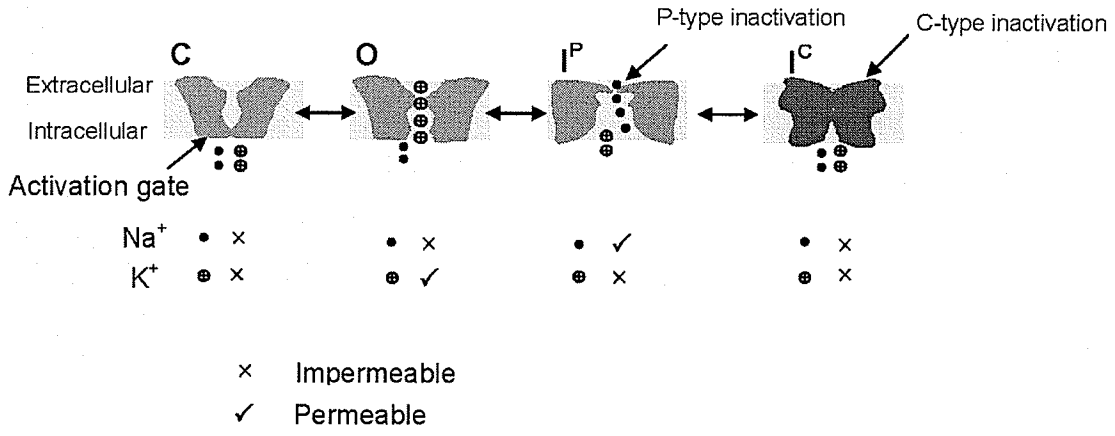

Figure 16. Proposed hERG gating scheme. I^P is the only state that conducts Na^+.

hERG gating scheme in Fig. 16 is supported by our experiments performed by using a pipette solution containing 135 mM Na^+ and a bath solution containing 1 mM K^+ (plus 135 mM NMG^+, Fig. 7). We have demonstrated that the hERG channel displayed its unique fast voltage dependent inactivation and recovery from inactivation when a K^+ free, Na^+ rich intracellular solution was used (Fig. 6 and 7). During the depolarizing step in Fig. 7A, an outward Na^+ current was observed. Upon repolarization, the inward K^+ currents were initially small and then increased in amplitude prior to deactivation. The

rising phase of the hERG K^+ tail current reflects the fast inactivated (I^P) channels quickly recovering to the open state and then deactivating (recovery from I^P is faster than deactivation). This result indicates that the Na^+ permeating state during depolarizing steps is the I^P. We have also demonstrated that the Na^+ current decays during prolonged depolarizing steps. This current decay may reflect the slow entry into the more stable inactivated state I^C from which recovery is slow (Fig. 4 and 5). Further insight regarding the Na^+ permeation state was also obtained from the F627Y mutant channel. Since the F627Y mutation removed the external Na^+ blocking effect, the inward Na^+ tail current could be recorded (Fig. 13 and 15). The F627Y Na^+ tail current upon repolarization did not display a rising phase (Fig. 15A). Yet, during repolarization, the I^P-inactivated F627Y channels recover to open before deactivation as evidenced by the rising phase of the inward K^+ tail current (Fig. 15B). Thus, the absence of the rising phase of the Na^+ current indicates that the Na^+ permeating state is not the open state. The absence of Na^+ permeation through the open hERG channels is also supported by the experiments shown in Fig. 4 C&D. After a large outward Na^+ current was induced by a depolarization to 70 mV, changing depolarizing voltage to less positive voltages induces a quick decay of the Na^+ currents, reflecting the fact that some channels are exiting the inactivated state and are transitioning into the open state. Consistently, the time constants of this fast decay are in millisecond ranges similar to the time constants of recovery from inactivation shown in Fig. 7. As well, in the S631A inactivation-deficient channels, depolarization failed to evoke any Na^+ current. However, the S631A channels were apparently in the open state during the depolarizing pulse since adding 1 mM K^+ to the bath solution caused a large inward tail current which occurred immediately upon repolarization without a rising

phase (Fig. 11). These results suggest that Na^+ does not significantly permeate through open channels.

We conclude that Na^+ permeates through the I^P-inactivated channels but not through the closed (resting), open or I^C-inactivated channels. We have found that the channel inactivation rate has been accelerated by 6.1-12.6 folds in T623A, F627Y and S641A mutations (Fig. 9). We have also found that the activation time course of the S641A Na^+ current was not different from that of WT currents, and the activation time courses of the T623A and F627Y Na^+ currents were slower than that of WT Na^+ currents (Fig. 10C). The slowed activation rate in T623A and F627Y mutants, which displayed accelerated inactivation, indicates that hERG channel does not directly enter into the inactivated state from the closed state. Instead, hERG channel must go through the open state to enter into inactivation states. Consistently, because onset of hERG P-type inactivation is much faster than for channel activation (Fig. 3, 7, 9 and 10), the rate-limit step of activation rates of the Na^+ currents are likely determined by the closed to open transition.

The concept that the I^P-inactivated state is the Na^+ permeating state is consistent with the data from *Shaker* channels. It was reported that the permeability of Na^+ ions through the open K^+ channel is negligible. However, the permeation properties change during inactivation and favor Na^+ permeation (Starkus et al., 1997a; Wang et al., 2000; Zhang et al., 2003b). It has been shown that the high Na^+ permeability state is an intermediate state between the open and deep 'C-type' inactivated states in Kv1.5 channels (Wang et al., 2000).

There are some differences between *Shaker* and hERG K^+ current inactivation. The onset of *Shaker* C-type inactivation is slower than that of hERG and is not obviously voltage dependent (Rasmusson et al., 1998). In contrast, the onset of inactivation of hERG is very fast and strongly voltage-dependent (Smith et al., 1996; Spector et al., 1996). The difference between hERG and *Shaker* inactivation may be due to the fact that hERG has a more flexible pore. There are 43 amino acids in hERG S5-P linker whereas there are only 14 to 18 amino acids in the corresponding region of most other Kv channels (Dun et al., 1999). In addition, the *Shaker* sequence has double tryptophans (WW) at the N-terminal end of the pore-loop, and a tyrosine (Y) in the "signature motif" (GYG) at the C-terminal end. According to the crystal structure of KcsA, a model K^+ channel, hydrogen bonds can be formed in the 3-dimensional structure around the outer mouth between the nitrogens of "WW" and the hydroxyl group of "Y" of the four subunits. These hydrogen bonds serve as "molecular springs", that pull the pore wall radially outward to hold the outer mouth open at its proper diameter (Doyle et al., 1998). Such hydrogen bonds seem so important that a single mutation of tryptophan to phenylalanine in *Shaker* (ShH4-IR W434F) or Kv1.5 (W472F) makes these channels nonconductive to K^+ due to the extremely fast entry into an inactivated state perhaps equivalent to I^P (Perozo et al., 1993; Chen et al., 1997; Yang et al., 1997b). Whereas no K^+ current would be detected, Na^+ current was present in the W434F Shaker and W472F Kv1.5 channels (Starkus et al., 1998; Wang and Fedida, 2002). As mentioned, the W434F *Shaker* and W472F Kv1.5 are not in a charge-immobilized I^C equivalent state. The corresponding tryptophans and tyrosine are missing in hERG. The absence of hydrogen bonds and long S5-P linker may lead to a more flexible pore (Tseng, 2001). Consequently, hERG channels are more prone

to enter into the less stable P-type inactivated state I^P. Recently, Berneche and Roux presented a model which couples the rate of inactivation with ion occupancy of the selectivity filter (Berneche et al., 2005). According to the model, there is a modest rearrangement that leads to a nonconducting conformational state of the selectivity filter, which is then effectively acting as a gate. This structural rearrangement involves only one of the four subunits at a time, breaking the 4-fold symmetry of the channel. The first step, which initiates the conformational transition toward the nonconducting state, is very sensitive to the configurations of the ion occupying the selectivity filter. Membrane depolarization (positive voltage shift) favors a state in which the transition can take place, and membrane polarization (negative voltage shift) favors a state which prevents the transition. This model could potentially explain the voltage dependence of hERG inactivation (Berneche et al., 2005). However, the voltage dependence of inactivation is not generally obvious in *Shaker*-related K^+ channels (Rasmusson et al., 1998). The lack of strong voltage dependence of the typical C-type inactivation of *Shaker* channels may be due to the hydrogen bonds between the tyrosine from the GYG moiety and a tryptophan from an adjacent subunit, corresponding to Tyr78 and Trp68 in KcsA, which offset the voltage dependence of the structural rearrangement leading to the nonconducting conformation state.

While the I^P inactivation may correspond to the fast inactivation in K^+ current recordings, I^C inactivation of hERG has not been described in the K^+ current recordings. It is known that external K^+ inhibits P/C-type inactivation (Zhang et al., 2003b; Zhang et al., 2003a; Zhang et al., 2005). It has been reported (Sanguinetti et al., 1995; Yang et al., 1997a) and

we have confirmed (Fig. 8) that reduction of K^+_o significantly decreases hERG current amplitude. Although lowering K^+_o accelerates the fast inactivation of hERG channels (Wang et al., 1996b; Wang et al., 1997; Zhang et al., 2003a), and this effect was initially thought to be responsible for the effect of K^+_o on the hERG current magnitude (Yang et al., 1997a), a quantitative analysis by Wang et al. suggested that the changed fast-inactivation rate is not responsible for the altered current amplitude (Wang et al., 1997). Presently, the mechanism of K^+_o-dependent changes of the hERG current amplitude is not known, and we believe that the entry into the slow 'C-type' inactivation at low K^+_o is responsible for this phenomenon as supported by our data shown in Fig. 8.

The reason why fast inactivated hERG channels are not permeable to K^+ but permeable to Na^+ is not known. It seems that the conformational change of the Serine side chain at 631 during inactivation is involved. Previously, Ulens and colleagues have reported that 250 μM norpropoxyphene, the major metabolite of propoxyphene, increased Na^+/K^+ permeability ratio by 30 folds in WT hERG channels but not in S631C mutant channels (Ulens et al., 1999), suggesting that norpropoxyphene may interact with S631 to increase the permeability ration of Na^+ over K^+. Fan *et al.* reported that S631K and S631E mutations significantly increased the hERG Na^+/K^+ permeability ratio (Fan et al., 1999). Therefore, we believe that the inactivation-associated conformational change of the Ser-631 may contribute to the increased Na^+ permeability during the inactivation process. This notion is also consistent with our data that there is no detectable Na^+ current in the S631A mutant channel (Fig. 11).

In WT hERG channels, while robust outward Na^+ current was recorded with a pipette solution containing 135 mM Na^+ and a bath solution containing 135 mM NMG^+ (Fig. 1-5), no Na^+ current could be detected when a 135 mM Na^+-containing bath solution was used. We found that external Na^+ potently blocks the Na^+ current in a concentration dependent manner (IC_{50} = 3.5 mM, Fig. 12). The Na^+_o block of hERG K^+ currents has been reported previously (Mullins et al., 2002), and the IC_{50} value for Na^+_o to block the hERG Na^+ current is close to that for Na^+_o to block hERG K^+ currents (Mullins et al., 2002). It was also reported that the S624A and S624T mutations removed the Na^+_o blocking effect on the hERG K^+ current (Mullins et al., 2002). It was proposed that Na^+_o induced block resulted from the competition between extracellular sodium and potassium for binding to the hERG channel pore, and that mutations of S624A and S624T increased the K^+ occupancy of the most outer pore site which resulted in both impaired inactivation and decreased sensitivity to inhibition by Na^+_o in the two mutant channels (Mullins et al., 2002). In the present study, we found that the S624A mutation also removed Na^+_o block of the hERG Na^+ current. Further, we found that the F627Y and S641A removed Na^+_o blocking effects on the hERG Na^+ current as well. Since the F627Y and S641A mutations significantly accelerated hERG inactivation, whereas S624A slightly decelerated it (data not shown, also see (Mullins et al., 2002)), inactivation gating seems not involved in the Na^+_o block of hERG channels. Also, since our experiments were performed in the absence of K^+, it ruled out any potential competition between Na^+_o and K^+_o for the binding to the hERG channel pore as a mechanism for Na^+_o induced hERG block. In the paper published by Mullins *et al*, it was also mentioned that Na^+ current through hERG channels could not be detected (Mullins et al., 2002). The reason for the discrepancy is

not known but may be related to the Na^+_o blocking effect. The exact mechanism of Na^+_o block of hERG Na^+ current is not known. It seems that the binding domain is located in the outer mouth of the channel pore since only external Na^+ can produce blocking effects. Mutations at the S624, F627 or S641 position of hERG may induce a conformational change that disrupts the binding domain for Na^+_o.

Although Na^+_o blocked hERG Na^+ current, a robust outward hERG Na^+ current indicates that intracellular Na^+ (Na^+_i) does not block the channels. This is in contrast to the effects of Na^+ ions on other voltage gated K^+ channels. Na^+_i is known to block several voltage-gated K^+ channels including rat ether-a-go-go (rEAG K^+ channel) (Pardo et al., 1998; Yellen, 1984; Pusch et al., 2001). On the other hand, Na^+_o generally does not block voltage-gated K^+ channels (Hille, 2001). Similarly, Na^+_i but not Na^+_o blocks the bacterial channel KcsA in lipid bilayers and the K^+-selective prokaryotic glutamate receptor GluR0. Sidedness of Na^+ block in these channels have been used to determine the channel topology (Heginbotham et al., 1999; Chen et al., 1999a). Clearly, Na^+ block of hERG channels displayed a sidedness opposite to that of most K^+ channels. The mechanisms of Na^+ block of hERG channels need further investigation.

In conclusion, by studying the Na^+ currents in hERG channels, we propose that there are at least two distinct inactivated states in hERG channels, the initial P-type and the more stable 'C-type' inactivated state. The Na^+ permeation and block of hERG channels provide a novel way to extend our understanding of hERG channel gating and modulation.

VII. CONCLUSION

1. We have discovered that Na^+ permeates through hERG K^+ channels.
2. We have identified that an inactivated state of the hERG channel is the only state that permeates Na^+.
3. Using the Na^+ permeation property, we have found that inactivation of the hERG channel involves at least two steps, the fast entry into the less stable; P-type inactivated state, and the slow entry into the more stable 'C-type' inactivated state. Na^+ permeates through the fast inactivated state (P-type) but not through either open state or 'C-type' inactivated state. The onset and recovery from P-type inactivation is fast, while the onset and recovery from 'C-type' inactivation is slow. The Na^+ current decay during depolarizations reflects the entry of the P-type inactivated channels into the 'C-type' inactivated state.
4. We also found that external Na^+ blocks the hERG Na^+ current with an IC_{50} of 3.5 mM.
5. Characterization of Na^+ permeation and block of hERG channels not only extends our understanding of hERG channel function and regulation but also provides a powerful tool for further investigation of hERG function and drug-hERG interactions.

VIII. FUTURE DIRECTIONS and CLINICAL RELEVANCE

hERG has received tremendous attention since its discovery in 1994 because inherited mutations or drug-induced blockade of channels increases the risk of lethal arrhythmia. Despite intense scrutiny, many issues regarding the physiological functions and mechanisms of gating, especially inactivation gating, of hERG channels remain unresolved.

Using the Na^+ permeation property, we have found that hERG channel inactivation involves at least two steps, the fast entry into the P-type inactivated state, and the slow entry into the stable 'C-type' inactivated state. The existence of 'C-type' inactivated state of the hERG channel provides us with valuable clues to investigate the physiological functions of the channel. We found that reduction of external concentration of K^+ ($[K^+_o]$) significantly decreases hERG K^+ current amplitude. Although the mechanism of K^+_o-dependent changes of the hERG current amplitude is not known, we believe that the entry into the slow 'C-type' inactivation at low K^+_o is responsible for this phenomenon. These studies suggested that changes in hERG K^+ current amplitude may occur in vivo as a result of small changes in $[K^+_o]$ asscociated with pathological (and perhaps physiological) conditions. In other words, $[K^+_o]$ controls the population of functional hERG channels which does not reside in the 'C-type' inactivated state. Studies on K^+ channel blockers, such as class III antiarrhythmia agents (hERG channel blockers), revealed that these intracellular channel blockers reduce K^+ occupancy of the channel pore (Valenzuela et al., 1995; Choi et al., 1999). Whether the reduction of K^+ occupancy induced by the channel

blockers leads to the channel to enter into the 'C-type' inactivation state needs to be further investigated. With the wide variety of drug blockers of the hERG channel being discovered, it will be of great interest to determine whether any of these drugs block the channel via modulation of K^+-sensitivity conformational changes.

IX. Reference List

Almers,W. and C.M.Armstrong. 1980. Survival of K^+ permeability and gating currents in squid axons perfused with K^+-free media. *J Gen Physiol* 75:61-78.

Armstrong,C.M. 1971. Interaction of tetraethylammonium ion derivatives with the potassium channels of giant axon. *J Gen Physiol* 58:413-437.

Balser,J.R., H.B.Nuss, N.Chiamvimonvat, M.T.Pérez-García, E.Marban, and G.F.Tomaselli. 1996. External pore residue mediates slow inactivation in μ1 rat skeletal muscle sodium channels. *J Physiol (Camb)* 494:431-442.

Barhanin,J., F.Lesage, E.Guillemare, M.Fink, M.Lazdunski, and G.Romey. 1996. K_vLQT1 and IsK (minK) proteins associate to form the I_{Ks} cardiac potassium current. *Nature* 384:78-80.

Berneche,S. and B.Roux. 2005. A gate in the selectivity filter of potassium channels. *Structure* 13:591-600.

Bezanilla,F., E.Perozo, and E.Stefani. 1994. Gating of *Shaker* K^+ channels: II. The components of gating currents and a model of channel activation. *Biophys J* 66:1011-1021.

Bian,J.S., J.Cui, Y.Melman, and T.V.McDonald. 2004. S641 contributes HERG K^+ channel inactivation. *Cell Biochem Biophys* 41:25-40.

Bianchi,L., B.Wible, A.Arcangeli, M.Taglialatela, F.Morra, P.Castaldo, O.Crociani, B.Rosati, L.Faravelli, M.Olivotto, and E.Wanke. 1998. HERG encodes a K^+ current highly conserved in tumors of different histogenesis-a selective advantage for cancer cells. *Cancer Res* 58:815-822.

Bruggemann,A., L.A.Pardo, W.Stuhmer, and O.Pongs. 1993. Ether-a-go-go encodes a voltage-gated channel permeable to K^+ and Ca^{2+} and modulated by cAMP. *Nature* 365:445-448.

Chen,F.S.P., D.Steele, and D.Fedida. 1997. Allosteric effects of permeating cations on gating currents during K^+ channel deactivation. *J Gen Physiol* 110:87-100.

Chen,G.Q., C.Cui, M.L.Mayer, and E.Gouaux. 1999a. Functional characterization of a potassium-selective prokaryotic glutamate receptor. *Nature* 402:817-821.

Chen,J., G.Seebohm, and M.C.Sanguinetti. 2002. Position of aromatic residues in the S6 domain, not inactivation, dictates cisapride sensitivity of HERG and eag potassium channels. *Proc Natl Acad Sci U S A* 99:12461-12466.

Chen,J., A.R.Zou, I.Splawski, M.T.Keating, and M.C.Sanguinetti. 1999b. Long QT syndrome-associated mutations in the Per-Arnt-Sim (PAS) domain of HERG potassium channels accelerate channel deactivation. *J Biol Chem* 274:10113-10118.

Chiesa,N., B.Rosati, A.Arcangeli, M.Olivotto, and E.Wanke. 1997. A novel role for HERG K^+ channels: Spike-frequency adaptation. *J Physiol (Camb)* 501:313-318.

Choi,J.S., S.J.Hahn, D.J.Rhie, S.H.Yoon, Y.H.Jo, and M.S.Kim. 1999. Mechanism of fluoxetine block of cloned voltage-activated potassium channel Kv1.3. *J Pharmacol Exp Ther* 291:1-6.

Choi,K.L., R.W.Aldrich, and G.Yellen. 1991. Tetraethylammonium blockade distinguishes two inactivation mechanisms in voltage-activated K^+ channels. *Proc Natl Acad Sci USA* 88:5092-5095.

Curran,M.E., I.Splawski, K.W.Timothy, G.M.Vincent, E.D.Green, and M.T.Keating. 1995. A molecular basis for cardiac arrhythmia: *HERG* mutations cause long QT syndrome. *Cell* 80:795-803.

De Biasi,M., H.A.Hartmann, J.A.Drewe, M.Taglialatela, A.M.Brown, and G.E.Kirsch. 1993. Inactivation determined by a single site in K^+ pores. *Pflugers Arch* 422:354-363.

Delisle,B.P., B.D.Anson, S.Rajamani, and C.T.January. 2004. Biology of cardiac arrhythmias: ion channel protein trafficking. *Circ Res* 94:1418-1428.

Demo,S.D. and G.Yellen. 1991. The inactivation gate of the *Shaker* K^+ channel behaves like an open-channel blocker. *Neuron* 7:743-753.

Doyle,D.A., J.M.Cabral, R.A.Pfuetzner, A.L.Kuo, J.M.Gulbis, S.L.Cohen, B.T.Chait, and R.MacKinnon. 1998. The structure of the potassium channel: Molecular basis of K^+ conduction and selectivity. *Science* 280:69-77.

Dun,W., M.Jiang, and G.N.Tseng. 1999. Allosteric effects of mutations in the extracellular S5-P loop on the grating and ion permeation properties of the hERG potassium channel. *Pflugers Archiv European Journal of Physiology* 439:141-149.

Fan,J.S., M.Jiang, W.Dun, T.V.McDonald, and G.N.Tseng. 1999. Effects of outer mouth mutations on *hERG* channel function: A comparison with similar mutations in the *Shaker* channel. *Biophys J* 76:3128-3140.

Faravelli,L., A.Arcangeli, M.Olivotto, and E.Wanke. 1996. A HERG-like K^+ channel in rat F-11 DRG cell line: Pharmacological identification and biophysical characterization. *J Physiol (Camb)* 496:13-23.

Farrelly,A.M., S.Ro, B.P.Callaghan, M.A.Khoyi, N.Fleming, B.Horowitz, K.M.Sanders, and K.D.Keef. 2003. Expression and function of KCNH2 (HERG) in the human jejunum. *Am J Physiol Gastrointest Liver Physiol* 284:G883-G895.

Ferrer,T., J.Rupp, D.R.Piper, and M.Tristani-Firouzi. 2006. The S4-S5 linker directly couples voltage sensor movement to the activation gate in the human ether-a'-go-go-related gene (hERG) K+ channel. *J Biol Chem* 281:12858-12864.

Ficker,E., A.T.Dennis, L.Wang, and A.M.Brown. 2003. Role of the cytosolic chaperones Hsp70 and Hsp90 in maturation of the cardiac potassium channel HERG. *Circ Res* 92:e87-100.

Ficker,E., W.Jarolimek, and A.M.Brown. 2001. Molecular determinants of inactivation and dofetilide block in ether a-go-go (EAG) channels and EAG-related K^+ channels. *Mol Pharmacol* 60:1343-1348.

Ficker,E., W.Jarolimek, J.Kiehn, A.Baumann, and A.M.Brown. 1998. Molecular determinants of dofetilide block of HERG K^+ channels. *Circ Res* 82:386-395.

Furutani,M., M.C.Trudeau, N.Hagiwara, A.Seki, Q.M.Gong, A.F.Zhou, S.Imamura, H.Nagashima, H.Kasanuki, A.Takao, K.Momma, C.T.January, G.A.Robertson, and R.Matsuoka. 1999. Novel mechanism associated with an inherited cardiac arrhythmia - Defective protein trafficking by the mutant HERG (G601S) potassium channel. *Circulation* 99:2290-2294.

Gang,H. and S.Zhang. 2006. Na^+ permeation and block of HERG potassium channels. *J Gen Physiol* 128:55-71.

Gong,Q., D.R.Keeney, M.Molinari, and Z.Zhou. 2005. Degradation of trafficking-defective long QT syndrome type II mutant channels by the ubiquitin-proteasome pathway. *J Biol Chem* 280:19419-19425.

Guo,J., H.Gang, and S.Zhang. 2006. Molecular determinants of cocaine block of hERG potassium channels. *J Pharmacol Exp Ther* 317:865-874.

Haverkamp,W., G.Breithardt, A.J.Camm, M.J.Janse, M.R.Rosen, C.Antzelevitch, D.Escande, M.Franz, M.Malik, A.Moss, and R.Shah. 2000. The potential for QT prolongation and proarrhythmia by non-antiarrhythmic drugs: clinical and

regulatory implications. Report on a policy conference of the European Society of Cardiology. *Eur Heart J* 21:1216-1231.

Heginbotham,L., M.LeMasurier, L.Kolmakova-Partensky, and C.Miller. 1999. Single *Streptomyces lividans* K^+ channels: Functional asymmetries and sidedness of proton activation. *J Gen Physiol* 114:551-559.

Hille,B. 2001. Ionic channels of excitable membranes. 3 ed. Sinauer Associates Inc., Sunderland, Massachusetts.

Ho,S.N., H.D.Hunt, R.M.Horton, J.K.Pullen, and L.R.Pease. 1989. Site-directed mutagenesis by overlap extension using the polymerase chain reaction. *Gene* 77:51-59.

Holmgren,M., M.E.Jurman, and G.Yellen. 1996. N-type inactivation and the S4-S5 region of the Shaker K^+ channel. *J Gen Physiol* 108:195-206.

Holmgren,M., K.S.Shin, and G.Yellen. 1998. The activation gate of a voltage-gated K^+ channel can be trapped in the open state by an intersubunit metal bridge. *Neuron* 21:617-621.

Hoshi,T., W.N.Zagotta, and R.W.Aldrich. 1990. Biophysical and molecular mechanisms of *Shaker* potassium channel inactivation. *Science* 250:533-538.

Hoshi,T., W.N.Zagotta, and R.W.Aldrich. 1991. Two types of inactivation in *Shaker* K^+ channels: Effects of alterations in the carboxy-terminal region. *Neuron* 7:547-556.

Isacoff,E.Y., Y.N.Jan, and L.Y.Jan. 1991. Putative receptor for the cytoplasmic inactivation gate in the *Shaker* K^+ channel. *Nature* 353:86-90.

Jiang,Y., A.Lee, J.Chen, M.Cadene, B.T.Chait, and R.MacKinnon. 2002a. Crystal structure and mechanism of a calcium-gated potassium channel. *Nature* 417:515-522.

Jiang,Y., A.Lee, J.Chen, M.Cadene, B.T.Chait, and R.MacKinnon. 2002b. The open pore conformation of potassium channels. *Nature* 417:523-526.

Kagan,A., Z.H.Yu, G.I.Fishman, and T.V.McDonald. 2000. The dominant negative LQT2 mutation A561V reduces wild-type HERG expression. *J Biol Chem* 275:11241-11248.

Kaplan,W.D. and W.E.Trout, III. 1969. The behavior of four neurological mutants of Drosophila. *Genetics* 61:399-409.

Keating,M.T. and M.C.Sanguinetti. 2001. Molecular and cellular mechanisms of cardiac arrhythmias. *Cell* 104:569-580.

Kiss,L., J.LoTurco, and S.J.Korn. 1999. Contribution of the selectivity filter to inactivation in potassium channels. *Biophys J* 76:253-263.

Korn,S.J. and S.R.Ikeda. 1995. Permeation selectivity by competition in a delayed rectifier potassium channel. *Science* 269:410-412.

Kuryshev,Y.A., E.Ficker, L.Wang, P.Hawryluk, A.T.Dennis, B.A.Wible, A.M.Brown, J.Kang, X.L.Chen, K.Sawamura, W.Reynolds, and D.Rampe. 2005. Pentamidine-

induced long QT syndrome and block of hERG trafficking. *J Pharmacol Exp Ther* 312:316-323.

Lees-Miller,J.P., Y.Duan, G.Q.Teng, and H.J.Duff. 2000. Molecular determinant of high-affinity dofetilide binding to HERG1 expressed in Xenopus oocytes: involvement of S6 sites. *Mol Pharmacol* 57:367-374.

Lin,J., J.Guo, H.Gang, P.Wojciechowski, J.T.Wigle, and S.Zhang. 2005. Intracellular K^+ is required for the inactivation-induced high affinity binding of cisapride to HERG channels. *Mol Pharmacol* 68:855-865.

Loots,E. and E.Y.Isacoff. 1998. Protein rearrangements underlying slow inactivation of the *Shaker* K^+ channel. *J Gen Physiol* 112:377-389.

Lopez,G.A., Y.N.Jan, and L.Y.Jan. 1994. Evidence that the S6 segment of the *Shaker* voltage-gated K^+ channel comprises part of the pore. *Nature* 367:179-182.

Lopez-Barneo,J., T.Hoshi, S.H.Heinemann, and R.W.Aldrich. 1993. Effects of external cations and mutations in the pore region on C-type inactivation of Shaker potassium channels. *Recept Channels* 1:61-71.

Ludwig,J., H.Terlau, F.Wunder, A.Bruggemann, L.A.Pardo, A.Marquardt, W.Stuhmer, and O.Pongs. 1994. Functional expression of a rat homologue of the voltage gated either a go-go potassium channel reveals differences in selectivity and activation kinetics between the Drosophila channel and its mammalian counterpart. *EMBO J* 13:4451-4458.

Melishchuk,A., A.Loboda, and C.M.Armstrong. 1998. Loss of *Shaker* K channel conductance in 0 K^+ solutions: Role of the voltage sensor. *Biophys J* 75:1828-1835.

Mitcheson,J.S., J.Chen, M.Lin, C.Culberson, and M.C.Sanguinetti. 2000. A structural basis for drug-induced long QT syndrome. *Proc Natl Acad Sci U S A* 97:12329-12333.

Modell,S.M. and M.H.Lehmann. 2006. The long QT syndrome family of cardiac ion channelopathies: a HuGE review. *Genet Med* 8:143-155.

Morais Cabral,J.H., A.Lee, S.L.Cohen, B.T.Chait, M.Li, and R.MacKinnon. 1998. Crystal structure and functional analysis of the HERG potassium channel N terminus: a eukaryotic PAS domain. *Cell* 95:649-655.

Mullins,F.M., S.Z.Stepanovic, R.R.Desai, A.L.George, Jr., and J.R.Balser. 2002. Extracellular sodium interacts with the HERG channel at an outer pore site. *J Gen Physiol* 120:517-537.

Nakajima,T., T.Furukawa, T.Tanaka, Y.Katayama, R.Nagai, Y.Nakamura, and M.Hiraoka. 1998. Novel mechanism of HERG current suppression in LQT2: shift in voltage dependence of HERG inactivation. *Circ Res* 83:415-422.

Olcese,R., R.Latorre, L.Toro, F.Bezanilla, and E.Stefani. 1997. Correlation between charge movement and ionic current during slow inactivation in *Shaker* K^+ channels. *J Gen Physiol* 110:579-589.

Pardo,L.A., A.Bruggeman, J.Camacho, and W.Stühmer. 1998. Cell cycle-related changes in the conducting properties of r-eag K^+ channels. *J Cell Biol* 143:767-775.

Perozo,E., R.MacKinnon, F.Bezanilla, and E.Stefani. 1993. Gating currents from a non-conducting mutant reveal open-closed conformation in Shaker K^+ channels. *Neuron* 11:353-358.

Perry,M., M.J.de Groot, R.Helliwell, D.Leishman, M.Tristani-Firouzi, M.C.Sanguinetti, and J.Mitcheson. 2004. Structural determinants of HERG channel block by clofilium and ibutilide. *Mol Pharmacol* 66:240-249.

Pusch,M., L.Ferrera, and T.Friedrich. 2001. Two open states and rate-limiting gating steps revealed by intracellular Na+ block of human KCNQ1 and KCNQ1/KCNE1 K+ channels. *J Physiol* 533:135-143.

Rasmusson,R.L., M.J.Morales, R.C.Castellino, Y.Zhang, D.L.Campbell, and H.C.Strauss. 1995. C-type inactivation controls recovery in a fast inactivating cardiac K^+ channel (Kv1.4) expressed in *Xenopus* oocytes. *J Physiol (Camb)* 489:709-721.

Rasmusson,R.L., M.J.Morales, S.Wang, S.Liu, D.L.Campbell, M.V.Brahmajothi, and H.C.Strauss. 1998. Inactivation of voltage-gated cardiac K^+ channels. *Circ Res* 82:739-750.

Roden,D.M. and J.R.Balser. 1999. A plethora of mechanisms in the HERG-related long QT syndrome. Genetics meets electrophysiology. *Cardiovasc Res* 44:242-246.

Roden,D.M., R.Lazzara, M.Rosen, P.J.Schwartz, J.Towbin, and G.M.Vincent. 1996. Multiple mechanisms in the long-QT syndrome. Current knowledge, gaps, and future directions. The SADS Foundation Task Force on LQTS. *Circulation* 94:1996-2012.

Sanguinetti,M.C., M.E.Curran, P.S.Spector, and M.T.Keating. 1996a. Spectrum of HERG K^+-channel dysfunction in an inherited cardiac arrhythmia. *Proc Natl Acad Sci USA* 93:2208-2212.

Sanguinetti,M.C., M.E.Curran, A.Zou, J.Shen, P.S.Spector, D.L.Atkinson, and M.T.Keating. 1996b. Coassembly of K_vLQT1 and minK (IsK) proteins to form cardiac I_{Ks} potassium channel. *Nature* 384:80-83.

Sanguinetti,M.C., C.Jiang, M.E.Curran, and M.T.Keating. 1995. A mechanistic link between an inherited and an acquired cardiac arrhythmia: *HERG* encodes the I_{Kr} potassium channel. *Cell* 81:299-307.

Sanguinetti,M.C. and N.K.Jurkiewicz. 1990a. Lanthanum blocks a specific component of I_K and screens membrane surface charge in cardiac cells. *Am J Physiol Heart Circ Physiol* 259:H1881-H1889.

Sanguinetti,M.C. and N.K.Jurkiewicz. 1990b. Two components of delayed rectifier K+ current: differential sensitivity to black by class III antiarrhythmic agents. *J Gen Physiol* 96:195-215.

Schönherr,R. and S.H.Heinemann. 1996. Molecular determinants for activation and inactivation of HERG, a human inward rectifier potassium channel. *J Physiol (Camb)* 493:635-642.

Schwartz,P.J. 1997. The long QT syndrome. *Curr Probl Cardiol* 22:297-351.

Smith,G.A., H.W.Tsui, E.W.Newell, X.Jiang, X.P.Zhu, F.W.Tsui, and L.C.Schlichter. 2002. Functional up-regulation of HERG K+ channels in neoplastic hematopoietic cells. *J Biol Chem* 277:18528-18534.

Smith,P.L., T.Baukrowitz, and G.Yellen. 1996. The inward rectification mechanism of the HERG cardiac potassium channel. *Nature* 379:833-836.

Spector,P.S., M.E.Curran, A.R.Zou, and M.C.Sanguinetti. 1996. Fast inactivation causes rectification of the I_{Kr} channel. *J Gen Physiol* 107:611-619.

Starkus,J.G., L.Kuschel, M.D.Rayner, and S.H.Heinemann. 1997a. Ion conduction through C-type inactivated *Shaker* channels. *J Gen Physiol* 110:539-550.

Starkus,J.G., L.Kuschel, M.D.Rayner, and S.H.Heinemann. 1998. Macroscopic Na^+ currents in the "nonconducting" *Shaker* potassium channel mutant W434F. *J Gen Physiol* 112:85-93.

Starkus,J.G., M.D.Rayner, and S.H.Heinemann. 1997b. Anomalous conduction in the "non-conducting Shaker K^+ channel mutant W434F. *Biophys J* 72:A232.

Stefani,E., L.Toro, E.Perozo, and F.Bezanilla. 1994. Gating of *Shaker* K^+ channels: I. Ionic and gating currents. *Biophys J* 66:996-1010.

Stühmer,W., F.Conti, M.Stocker, O.Pongs, and S.H.Heinemann. 1991. Gating currents of inactivating and non-inactivating potassium channel expressed in Xenopus oocytes. *Pflugers Arch* 410:423-429.

Tristani-Firouzi,M., J.Chen, J.S.Mitcheson, and M.C.Sanguinetti. 2001. Molecular biology of K(+) channels and their role in cardiac arrhythmias. *Am J Med* 110:50-59.

Trudeau,M.C., J.W.Warmke, B.Ganetzky, and G.A.Robertson. 1995. HERG, a human inward rectifier in the voltage-gated potassium channel family. *Science* 269:92-95.

Tseng,G.N. 2001. I_{Kr}: The hERG channel. *J Mol Cell Cardiol* 33:835-849.

Ulens,C., P.Daenens, and J.Tytgat. 1999. Norpropoxyphene-induced cardiotoxicity is associated with changes in ion-selectivity and gating of HERG currents. *Cardiovasc Res* 44:568-578.

Valenzuela,C., E.Delpón, M.M.Tamkun, J.Tamargo, and D.J.Snyders. 1995. Stereoselective block of a human cardiac potassium channel (Kv1.5) by bupivacaine enantiomers. *Biophys J* 69:418-427.

Wang,J.L., M.C.Trudeau, A.M.Zappia, and G.A.Robertson. 1998. Regulation of deactivation by an amino terminal domain in *human ether-a-go-go-related gene* potassium channels. *J Gen Physiol* 112:637-647.

Wang,Q., M.E.Curran, I.Splawski, T.C.Burn, J.M.Millholland, T.J.VanRaay, J.Shen, K.W.Timothy, G.M.Vincent, T.De Jager, P.J.Schwartz, J.A.Towbin, A.J.Moss, D.L.Atkinson, G.M.Landes, T.D.Connors, and M.T.Keating. 1996a. Positional cloning of a novel potassium channel gene: *KVLQT1* mutations cause cardiac arrhythmias. *Nature Genet* 12:17-23.

Wang,Q., J.Shen, I.Splawski, D.Atkinson, Z.Li, J.L.Robinson, A.J.Moss, J.A.Towbin, and M.T.Keating. 1995. *SCN5A* mutations associated with an inherited cardiac arrhythmia, long QT syndrome. *Cell* 80:805-811.

Wang,S., M.J.Morales, S.Liu, H.C.Strauss, and R.L.Rasmusson. 1996b. Time, voltage and ionic concentration dependence of rectification of h-erg expressed in *Xenopus* oocytes. *FEBS Lett* 389:167-173.

Wang,S.M., S.G.Liu, M.J.Morales, H.C.Strauss, and R.L.Rasmusson. 1997. A quantitative analysis of the activation and inactivation kinetics of *HERG* expressed in *Xenopus* oocytes. *J Physiol (Camb)* 502:45-60.

Wang,S.Y. and G.K.Wang. 1997. A mutation in segment I-S6 alters slow inactivation of sodium channels. *Biophys J* 72:1633-1640.

Wang,Z. and D.Fedida. 2001. Gating charge immobilization caused by the transition between inactivated states in the Kv1.5 channel. *Biophys J* 81:2614-2627.

Wang,Z. and D.Fedida. 2002. Uncoupling of gating charge movement and closure of the ion pore during recovery from inactivation in the Kv1.5 channel. *J Gen Physiol* 120:249-260.

Wang,Z.R., J.C.Hesketh, and D.Fedida. 2000. A high-Na^+ conduction state during recovery from inactivation in the K^+ channel Kv1.5. *Biophys J* 79:2416-2433.

Warmke,J.W. and B.Ganetzky. 1994. A family of potassium channel genes related to eag in Drosophila and mammals. *Proc Natl Acad Sci U S A* 91:3438-3442.

Yang,T., D.J.Snyders, and D.M.Roden. 1997a. Rapid inactivation determines the rectification and $[K^+]_o$ dependence of the rapid component of the delayed rectifier K^+ current in cardiac cells. *Circ Res* 80:782-789.

Yang,Y.S., Y.Y.Yan, and F.J.Sigworth. 1997b. How does the W434F mutation block current in *Shaker* potassium channels. *J Gen Physiol* 109:779-789.

Yellen,G. 1984. Relief of Na^+ block of $Ca2^+$-activated K^+ channels by external cations. *J Gen Physiol* 84:187-199.

Zagotta,W.N. and R.W.Aldrich. 1990. Voltage-dependent gating of Shaker A-type potassium channels in Drosophila muscle. *J Gen Physiol* 95:29-60.

Zagotta,W.N., T.Hoshi, and R.W.Aldrich. 1990. Restoration of inactivation in mutants of *Shaker* potassium channels by a peptide derived from ShB. *Science* 250:568-571.

Zhang,J.-F., P.T.Ellinor, R.W.Aldrich, and R.W.Tsien. 1994. Molecular determinants of voltage-dependent inactivation in calcium channels. *Nature* 372:97-100.

Zhang,S., C.Eduljee, D.C.Kwan, S.J.Kehl, and D.Fedida. 2005. Constitutive Inactivation of the hKv1.5 Mutant Channel, H463G, in K^+-Free Solutions at Physiological pH. *Cell Biochem Biophys* 43:221-230.

Zhang,S., S.J.Kehl, and D.Fedida. 2003a. Modulation of human ether-a-go-go-related K^+ (HERG) channel inactivation by Cs^+ and K^+. *Journal of Physiology-London* 548:691-702.

Zhang,S., H.T.Kurata, S.J.Kehl, and D.Fedida. 2003b. Rapid induction of P/C-type inactivation is the mechanism for acid-induced K^+ current inhibition. *J Gen Physiol* 121:215-225.

Zhang,S., Z.Zhou, Q.Gong, J.C.Makielski, and C.T.January. 1999. Mechanism of block and identification of the verapamil binding domain to HERG potassium channels. *Circ Res* 84:989-998.

Zhou,Z., Q.Gong, B.Ye, Z.Fan, J.C.Makielski, G.A.Robertson, and C.T.January. 1998. Properties of HERG channels stably expressed in HEK 293 cells studied at physiological temperature. *Biophys J* 74:230-241.